REPORT No. 492

TESTS OF 16 RELATED AIRFOILS AT HIGH SPEEDS

By John Stack and Albert E. von Doenhoff

SUMMARY

In order to provide information that might lead to the development of better propeller sections, 13 related symmetrical airfoils have been tested in the N.A.C.A. high-speed wind tunnel for a study of the effect of thickness form on the aerodynamic characteristics.

The thickness-form variables studied were the value of the maximum thickness, the position along the chord at which the maximum thickness occurs, and the value of the leading-edge radius. A system of equations was used to define the airfoil forms so that fair profiles having systematic changes would be obtained. The basic thickness form is very nearly the same as that chosen for the recent investigation of a large number of related airfoils in the variable-density wind tunnel (N.A.C.A. Technical Report No. 460).

The tests were conducted through the low angle-of-attack range for speeds extending from 35 percent of that of sound to slightly in excess of the speed at which a compressibility burble, or breakdown of flow, occurs. The corresponding Reynolds Number range is 350,000 to 750,000. Because the Reynolds Number for the tests is somewhat lower than that at which most propellers operate, and much lower than that at which airplane wings operate, the data are not directly applicable to many practical problems, but it is probable that some of the relations shown, particularly the relative effect of the shape changes as affected by compressibility, are valid at much higher values of the Reynolds Number. The results obtained were applied to the design of three cambered airfoils which were tested as part of this investigation.

The principal factors affecting the choice of propeller sections are low drag at low and moderate lift coefficients and a late compressibility burble, that is, low drags at high speeds. Considering these factors, the results indicate that the maximum thickness should be small and located at approximately 40 percent of the chord aft of the leading edge. Small variations from the normal values for the leading-edge radius are shown to have small effect on the aerodynamic characteristics. A comparison with similar tests of commonly used propeller sections indicates that at high speeds one of the cambered airfoils tested, the N.A.C.A. 2409–34, is superior. The results also indicate that some further improvement in airfoil shapes for high-speed applications may be expected.

INTRODUCTION

Experimental investigations of the relationship between airfoil shapes and airfoil aerodynamic characteristics have generally been made at some particular dynamic scale, or Reynolds Number, and usually at relatively low speeds. Because the forces on an airfoil are affected by air compressibility, the speed at which tests are made may become an important parameter in the application of the results. It has been shown that the speed of flow expressed in terms of the speed of wave propagation, or the speed of sound, in the fluid is an index of the extent to which the flow is affected by compressibility. Thus, the ratio of the flow velocity to the velocity of sound, V/V_c, is a parameter indicative of flow pattern similarity in relation to compressibility effects just as the Reynolds Number is an index of the effects of viscosity. Therefore, if the speed at which the full-scale airfoil normally operates is greatly in excess of the speed at which the model was tested, the test results may be subject to a correction for the effects of compressibility.

The importance of the compressibility effect cannot be disregarded for many modern applications. Previous airfoil tests over wide speed ranges (see reference 1) indicated that for speeds in excess of 300 miles per hour the compressibility effect on the airfoil characteristics may be large. It is therefore necessary to investigate the relationship between airfoil shape and the aerodynamic characteristics at high speeds for such applications as the design of propellers, diving bombers, and high-speed racing airplanes.

The aerodynamic characteristics of airfoils may be considered as being dependent on the thickness-to-chord ratio (hereinafter referred to as the "thickness"), the thickness distribution, and the mean-line shape. The present investigation was made to study the effects of changes in the thickness and the thickness distribution on the aerodynamic characteristics of airfoils, particularly at high speeds, and to provide additional information for the study of compressibility phenomena. This information should lead to the design of better propeller sections. The effects of these changes were determined by tests over a wide speed range of 13 symmetrical airfoils having systematic changes of three variables. These variables are, for a fixed chord

length, the magnitude of the maximum thickness, the position of the maximum thickness, and the radius of the leading edge. Three cambered airfoils were also tested as a preliminary step in the investigation of the effects of mean-line shape on the aerodynamic characteristics at high speeds.

The tests consisted of the measurement of the lift, drag, and moment about the quarter-chord axis of the models for a range of speeds extending from about 35 percent of the speed of sound to speeds slightly in excess of the speed at which the breakdown of flow corresponding to the compressibility burble occurred. The tests were conducted in the N.A.C.A. high-speed wind tunnel during 1932–33.

DESCRIPTION OF AIRFOILS

The variables herein considered as determining the thickness form are the maximum thickness, the position of the maximum thickness, and the radius of the leading edge expressed in terms of the chord. These parameters determining the thickness form so expressed as ratios to the chord will throughout this report be referred to simply as "thickness", "position of maximum thickness", and "leading-edge radius." Arbitrary values of these three variables were so chosen as to provide systematic variations over the entire probable useful range of forms. The resulting airfoil forms were defined by means of a system of equations to insure fairness of the profiles, and the coefficients of the various terms of the equations were determined from conditions imposed by the assumed values of the independent variables. The basic form is shown in figure 1. On the same figure the basic thickness distribution used in the investigation in reference 2 is also shown. The leading-edge radius, the slope at the tail, the maximum thickness, the trailing-edge ordinate, and the position of the maximum thickness were made the same as those of the basic form given in reference 2, which has been designated the "N.A.C.A. 0020" airfoil.

Range of forms.—The range of forms investigated is shown by the airfoil design numbers in the following table:

DESIGN NUMBERS

0006–63	0009–33
0012–63	0009–93
0009–63	0009–05
0009–62	0009–35
0009–64	0009–34
0009–65	2209–34
0009–66	2409–34
0009–03	4409–34

In the design numbers given above, the first group of four digits gives the camber and thickness designation and has the same significance as the airfoil design numbers given in reference 1; that is, the first digit indicates the mean camber in percent of the chord; the second, the position of the camber in tenths of the chord aft of the leading edge; and the last two give the maximum thickness in percent of the chord. The group of digits following the dash designate the thickness distribution. The first digit designates the leading-edge radius and the second digit gives the position of the maximum thickness in tenths of the chord aft of the leading edge.

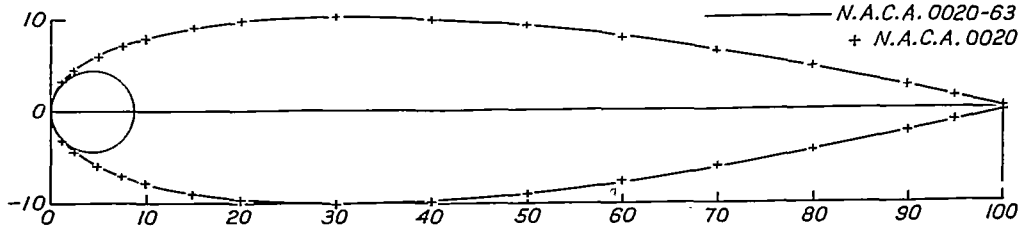

FIGURE 1.—Basic thickness distribution for airfoils tested in the high-speed wind tunnel (N.A.C.A. 0020-63) compared with basic thickness distribution for N.A.C.A. family airfoils (N.A.C.A. 0020, reference 2).

The significance of the leading-edge radius designation is given below:

- 0 designates sharp leading edge.
- 3 designates one-fourth normal leading-edge radius.
- 6 designates normal leading-edge radius (the leading-edge radius used in reference 2).
- 9 designates three times normal leading-edge radius or greater.

The leading-edge radius of the blunt-nosed airfoil used in this investigation is three times the normal value.

Thus, the N.A.C.A. 0009–64 is a 9 percent thick symmetrical airfoil having a normal leading-edge radius and its maximum thickness 40 percent of the chord aft of the leading edge. The N.A.C.A. 2409–34 airfoil has a maximum mean camber of 2 percent located at 40 percent of the chord, and is 9 percent thick. The leading-edge radius is one-fourth of the normal value and the maximum thickness is located at 40 percent of the chord aft of the leading edge.

The range of thickness ratios tested in this investigation was small because it was considered necessary to show only how relations already found for the effect of thickness variation at low speeds are affected by compressibility, and also because the airfoils chosen for high-speed application will of necessity be relatively thin. The value 09 of the maximum thickness ratio of the airfoils designed for the study of variables other than the maximum thickness was chosen because it is representative of the thickness range from which airfoil sections for propellers would probably be chosen. The airfoil profiles are shown in figure 2, and the ordinates are given in table I.

Derivation of new thickness forms.—The airfoil forms tested in this investigation have been defined by two equations. Two equations were used rather than a single equation, because a single-equation system led to shape differences aft of the position of maximum thickness when the leading-edge radius was changed and also led to reversals of curvature unless a very great number of terms were used.

If the chord is taken as the x axis from 0 to 1, the ordinates y from the leading edge to the position of maximum thickness are given by an equation of the form

$$\pm y = a_0\sqrt{x} + a_1 x + a_2 x^2 + a_3 x^3 \qquad (1)$$

The ordinates from the position of maximum thickness aft are given by an equation of the form

$$\pm y = d_0 + d_1(1-x) + d_2(1-x)^2 + d_3(1-x)^3 \qquad (2)$$

The coefficients of the equation for the forward portion are determined from the following conditions:

(a) Maximum thickness

$x=m$ $y=0.1$ (where m is the location of the maximum thickness in terms of the chord measured from the leading edge)

$$\frac{dy}{dx}=0$$

(b) Leading-edge radius

The leading-edge radius is derived from equation (1) and is $\frac{a_0^2}{2}$. Values of a_0 chosen to give certain desired leading-edge radii are shown in the following table:

Type	Index	a_0
Sharp	0	0
Quarter normal	3	0.148450
Normal	6	.296900
Three times normal	9	.514246

(c) Radius of curvature at the point of maximum thickness

Radius of curvature at $x=m$,

$$R=\frac{(1-m)^2}{2d_1(1-m)-0.588}$$

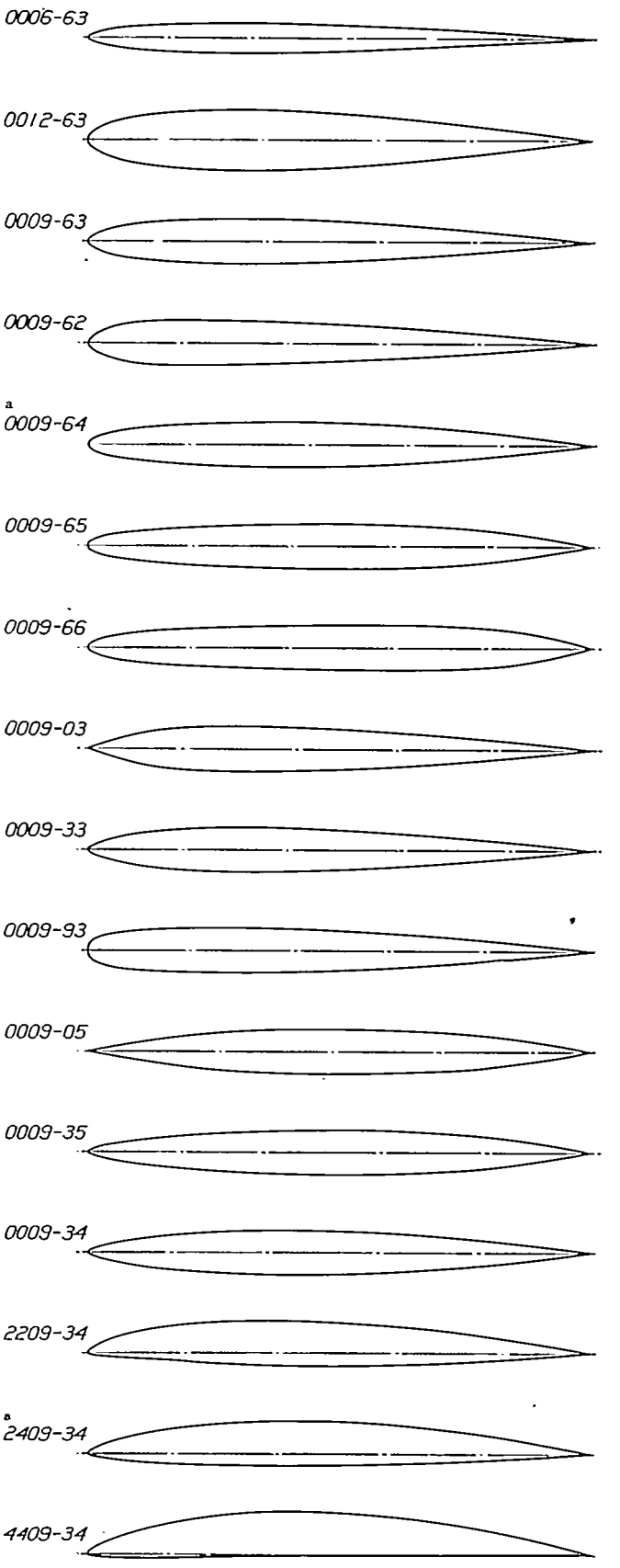

FIGURE 2.—Airfoil profiles.

[a] The N.A.C.A. 0009-64 has been previously referred to as the N.A.C.A. 204 and the N.A.C.A. 2409-34, as the N.A.C.A. 216.

(this value is derived from the equation for the after portion of the airfoil and is the same for both equations at $x=m$).

The conditions that were taken to determine the coefficients for the equation for the after portion are:

(a) Maximum thickness

$$x=m \qquad y=0.1 \qquad \frac{dy}{dx}=0$$

(b) Ordinate at trailing edge

$$x=1 \qquad y=d_0=0.002$$

(c) Trailing-edge angle

$$x=1 \qquad \frac{dy}{dx}=d_1=f(m)$$

The values of d_1 as a function of m, which were chosen to avoid reversals of curvature, are given in the following table:

m	d_1
0.2	0.200
.3	.234
.4	.315
.5	.465
.6	.700

Substitution of the coefficients derived from the foregoing conditions in equations (1) and (2) gives equations for symmetrical airfoils 20 percent thick. These coefficients are given in table II.

The airfoil ordinates for any other thickness are determined by multiplying the ordinates derived from the above equations by $\frac{t}{0.2}$, where t is the airfoil thickness expressed as a fraction of the chord. The leading-edge radius for any thickness is given by $\frac{1}{2}\left[\frac{t}{0.2}a_0\right]^2$.

Derivation of cambered airfoils.—The three cambered airfoils were derived by combining one of the best thickness forms, the 0009–34, with certain mean-line forms chosen from reference 2. The mean lines chosen have the 2200, 2400, and 4400 forms. The methods of combining the thickness distribution with the mean-line forms are given in detail in reference 2.

APPARATUS AND METHOD

Apparatus.—A complete description of the high-speed wind tunnel and a detailed account of the method of conducting tests are given in reference 1. The models used for this investigation were of 2-inch chord and were made of steel. The method of constructing the airfoils is described in reference 3.

Method of testing.—The tests consisted of the measurement of the lift, drag, moment, and dynamic pressure for several speeds in the range extending from 35 percent of the speed of sound to speeds slightly in excess of that at which the compressibility burble occurs. The corresponding Reynolds Number range is from 350,000 to 750,000. The angle-of-attack range for the tests of the symmetrical airfoils extended from −4° to 4°. The additional tests required to determine the maximum lift coefficients would have unnecessarily prolonged the testing program because inferior airfoils for high-speed applications can be detected by their earlier compressibility burble. The tests on the three cambered airfoils were conducted through the low angle-of-attack range, and one of the three which showed promise as a practical propeller section was chosen for tests throughout the complete angle-of-attack range. The order of the tests was arranged, as far as practicable, so that the tests to determine the effects of a single variable were made consecutively.

RESULTS

The test results are presented graphically in figures 3 to 18. Each figure presents complete data for one airfoil for the range of angle of attack tested. Each curve shows the variation of one of the coefficients with V/V_c for a given angle of attack. In the presentation of the moment-coefficient data the origin of the axes for each angle of attack has been raised above that for the previous angle of attack, so that the moment curve for any angle may be easily distinguished.

The data presented in figures 3 to 18 were cross-plotted in figures 19 to 34 to show the aerodynamic characteristics of the airfoils in the usual form. Figures 35 to 38 show the effect of the important shape variables on the aerodynamic characteristics. A comparison of the cambered airfoils is given in figures 39 and 40.

PRECISION

The various factors contributing to inaccuracy in these experiments may, in general, be classified under two divisions. The first consists of systematic and the second, of accidental errors. A detailed discussion of the probable systematic errors is given in reference 1.

The accidental errors are shown by the scattering of the points on the curves and by differences between original and check tests of the 0009–63 and 0009–65 airfoils. Errors in the angle of attack may be as large as ¼°, owing partly to errors in mounting the airfoils and partly to dissymmetry of the symmetrical airfoils. The balance and static-plate calibrations made before and after the tests checked to within 1.5 percent. Inaccuracies arising from other sources are within ± 0.005 for the lift coefficient, ± 0.0005 for the drag coefficient, and ± 0.002 for the moment coefficient. The errors in the results of the 0009–66 airfoil may be larger than the above-mentioned values because a special correction was applied to these data to account for the large dissymmetry of this airfoil.

DISCUSSION

The data have been analyzed to show primarily the effects of shape changes on airfoil aerodynamic characteristics at high speeds in order to provide information

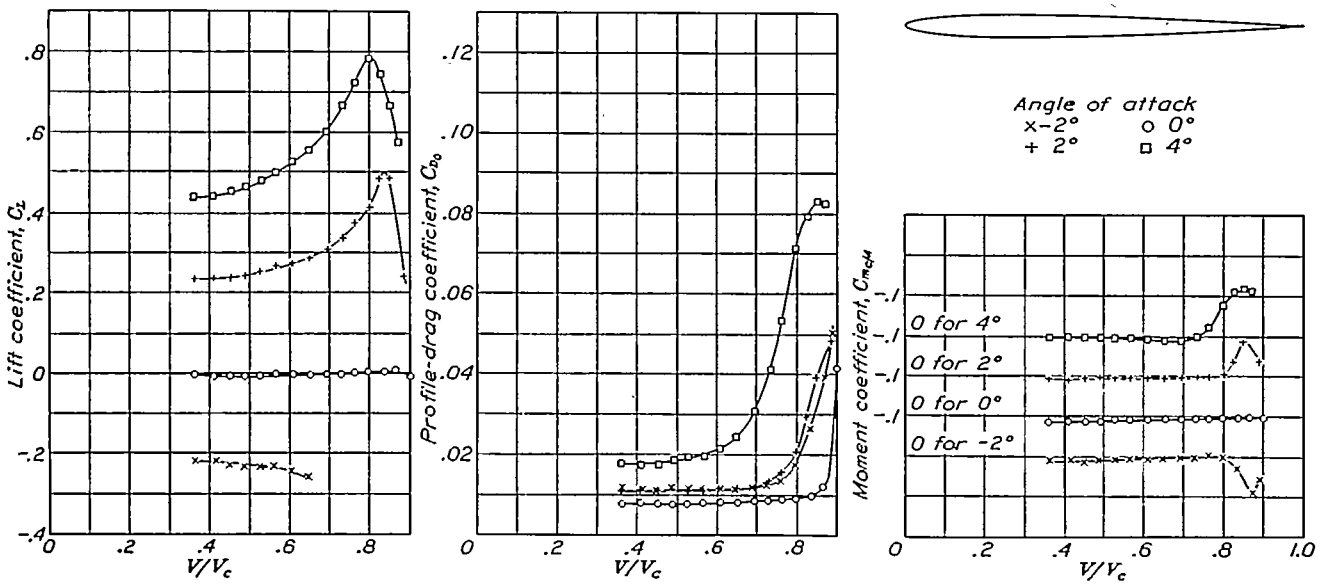

FIGURE 3.—Effect of compressibility on the aerodynamic characteristics of the N.A.C.A. 0006-63 airfoil.

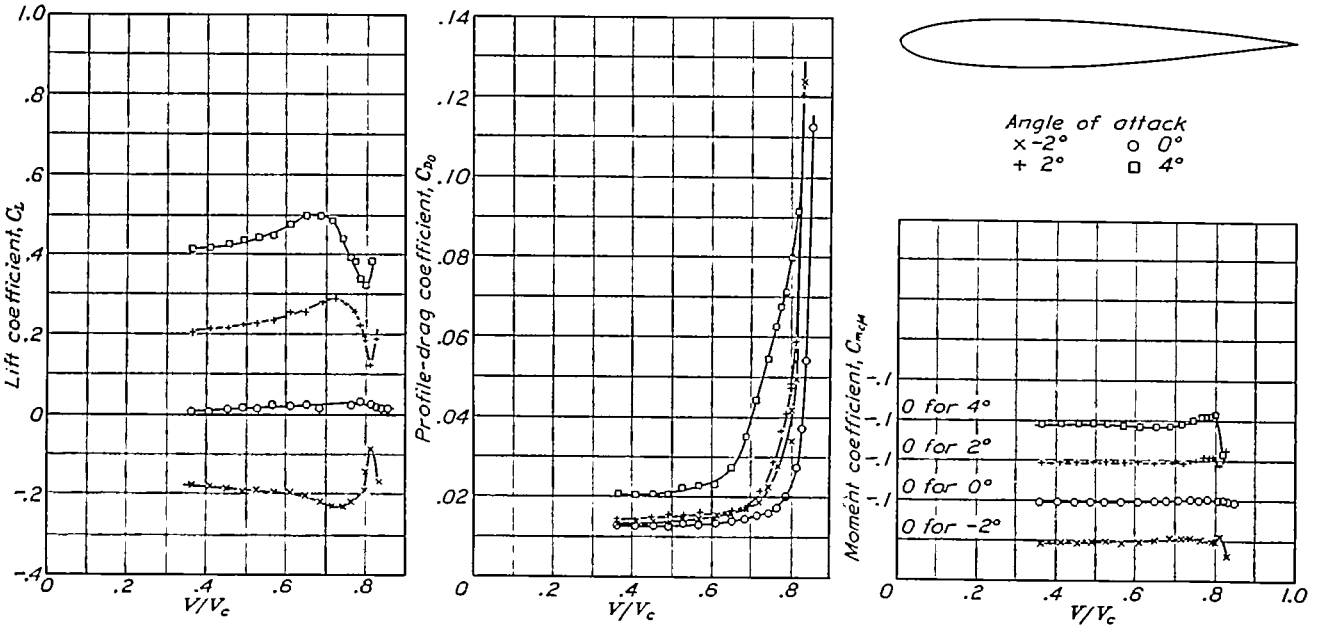

FIGURE 4.—Effect of compressibility on the aerodynamic characteristics of the N.A.C.A. 0012-63 airfoil.

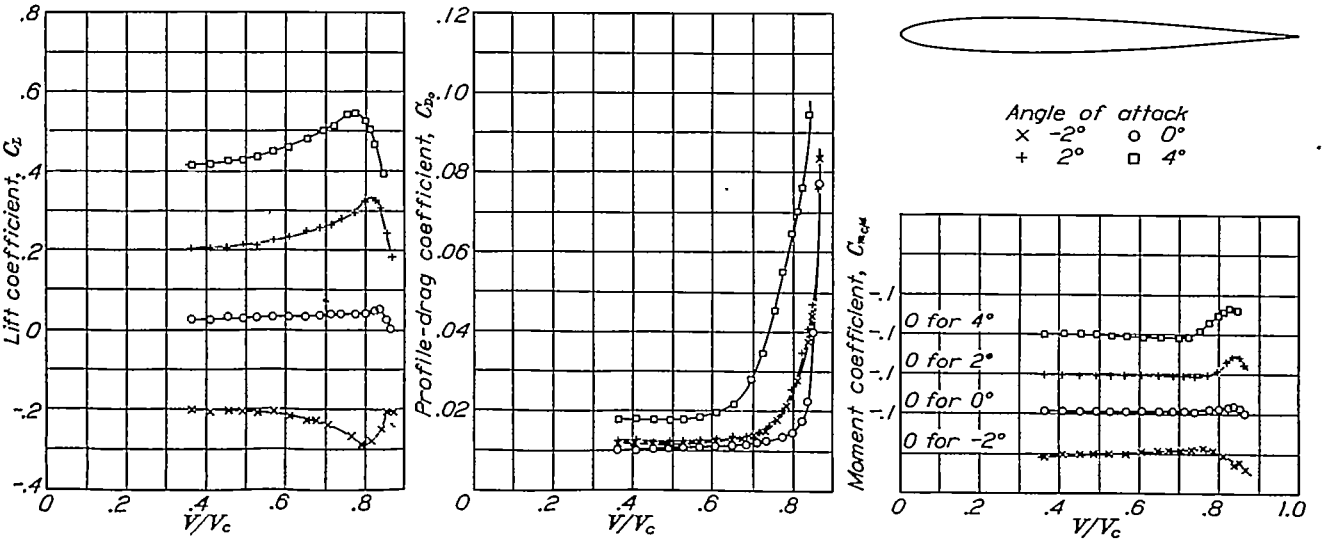

FIGURE 5.—Effect of compressibility on the aerodynamic characteristics of the N.A.C.A. 0009-63 airfoil.

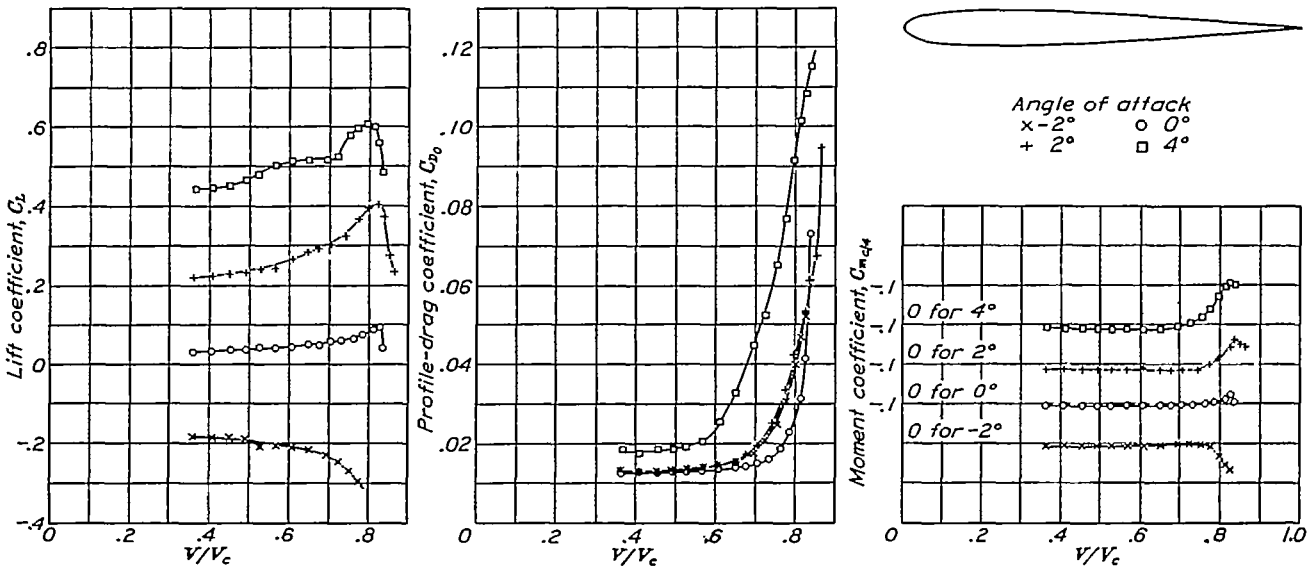

FIGURE 6.—Effect of compressibility on the aerodynamic characteristics of the N.A.C.A. 0009-62 airfoil.

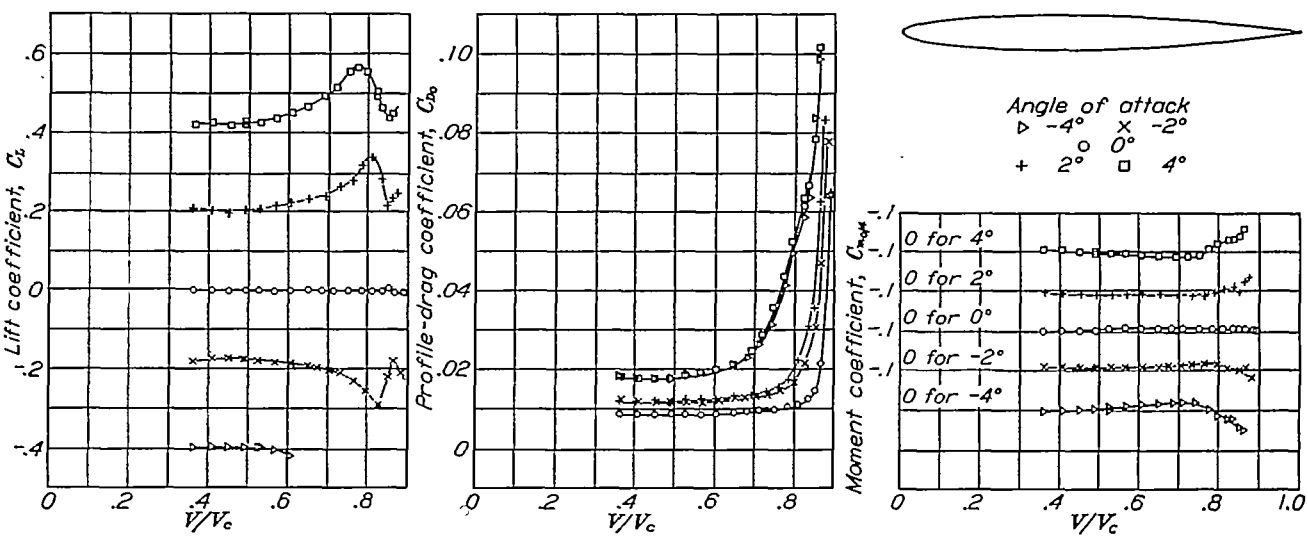

FIGURE 7.—Effect of compressibility on the aerodynamic characteristics of the N.A.C.A. 0009-64 airfoil.

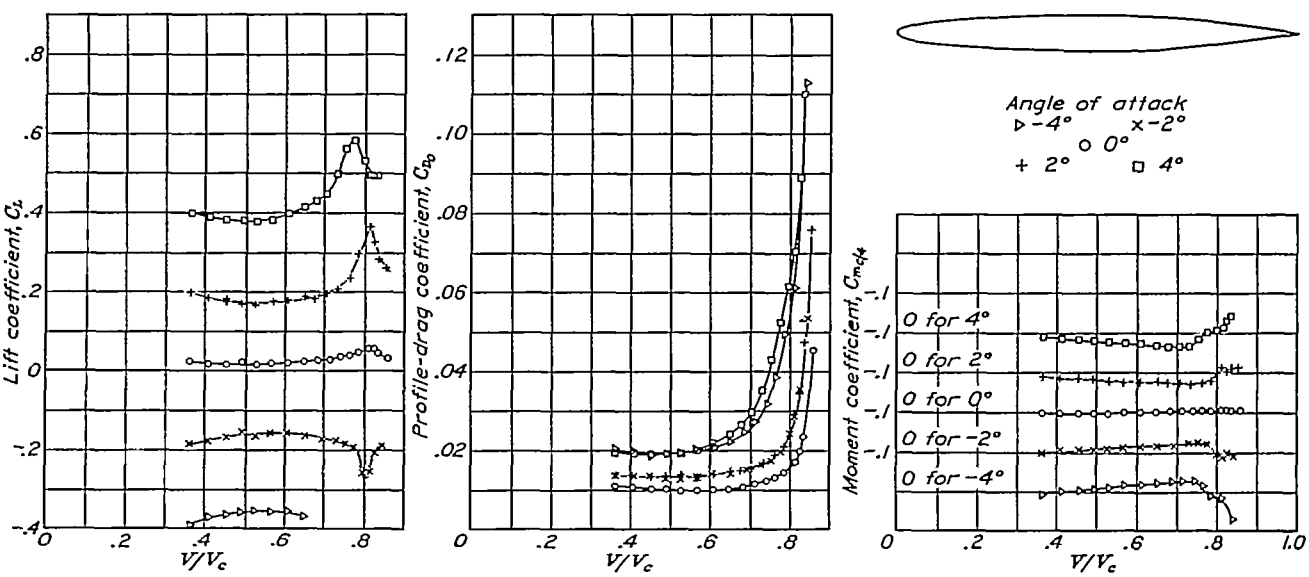

FIGURE 8.—Effect of compressibility on the aerodynamic characteristics of the N.A.C.A. 0009-65 airfoil.

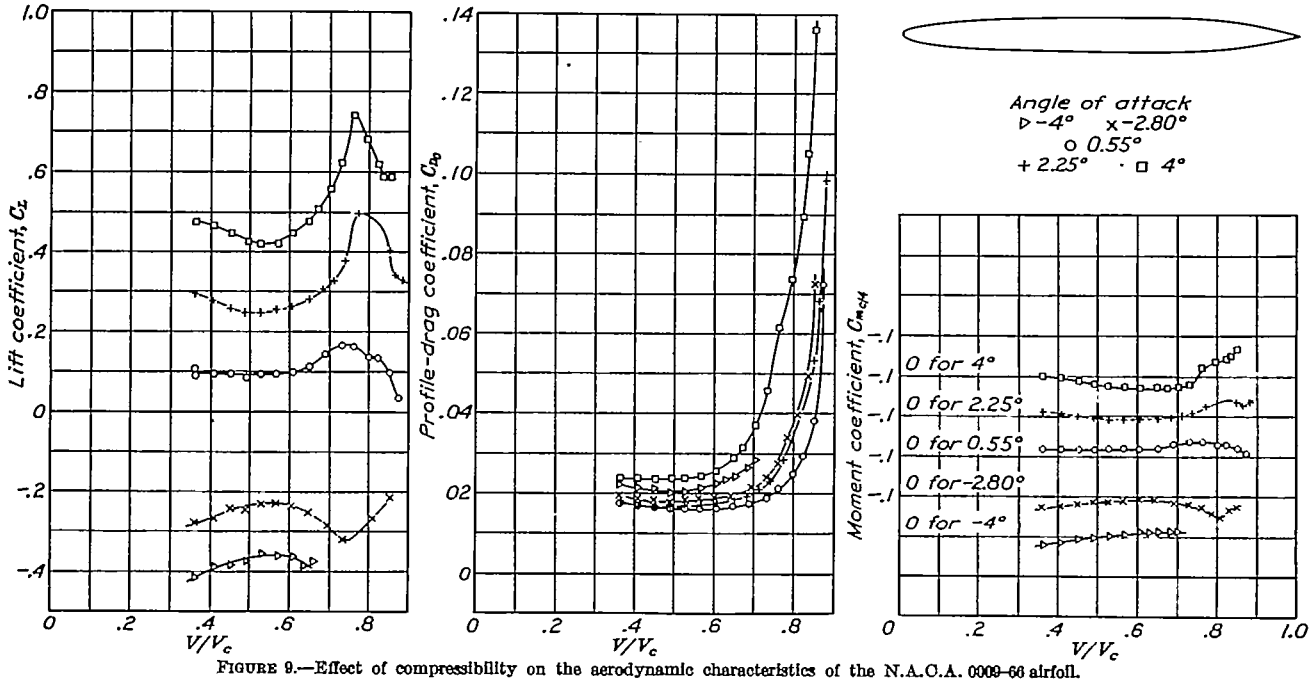

FIGURE 9.—Effect of compressibility on the aerodynamic characteristics of the N.A.C.A. 0009-66 airfoil.

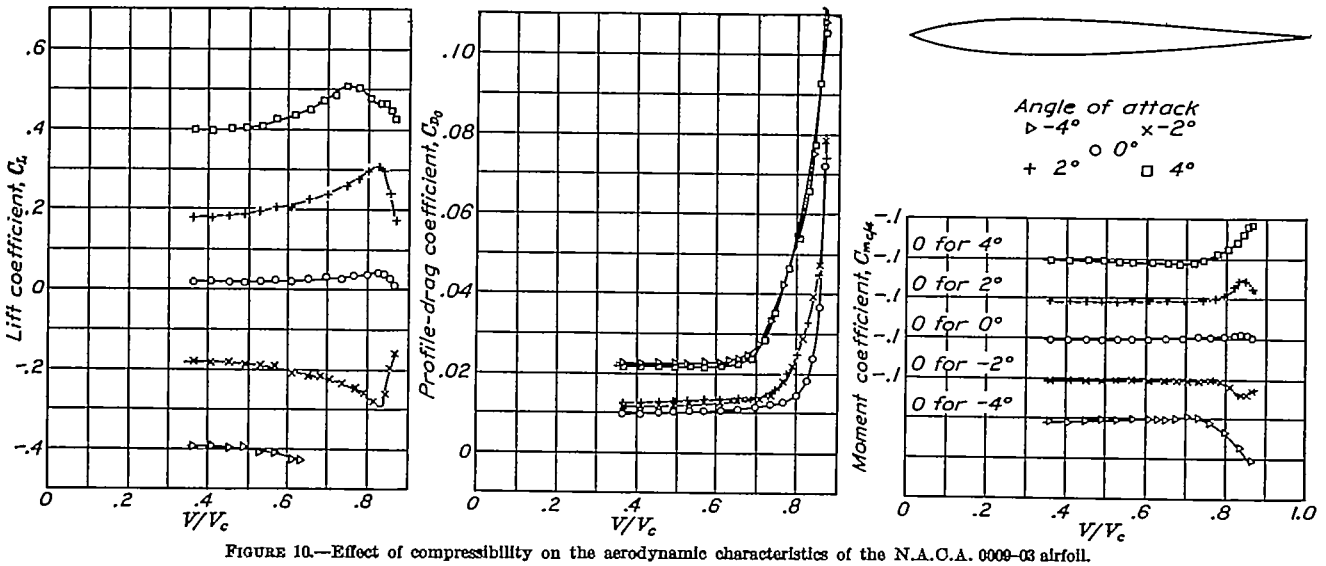

FIGURE 10.—Effect of compressibility on the aerodynamic characteristics of the N.A.C.A. 0009-03 airfoil.

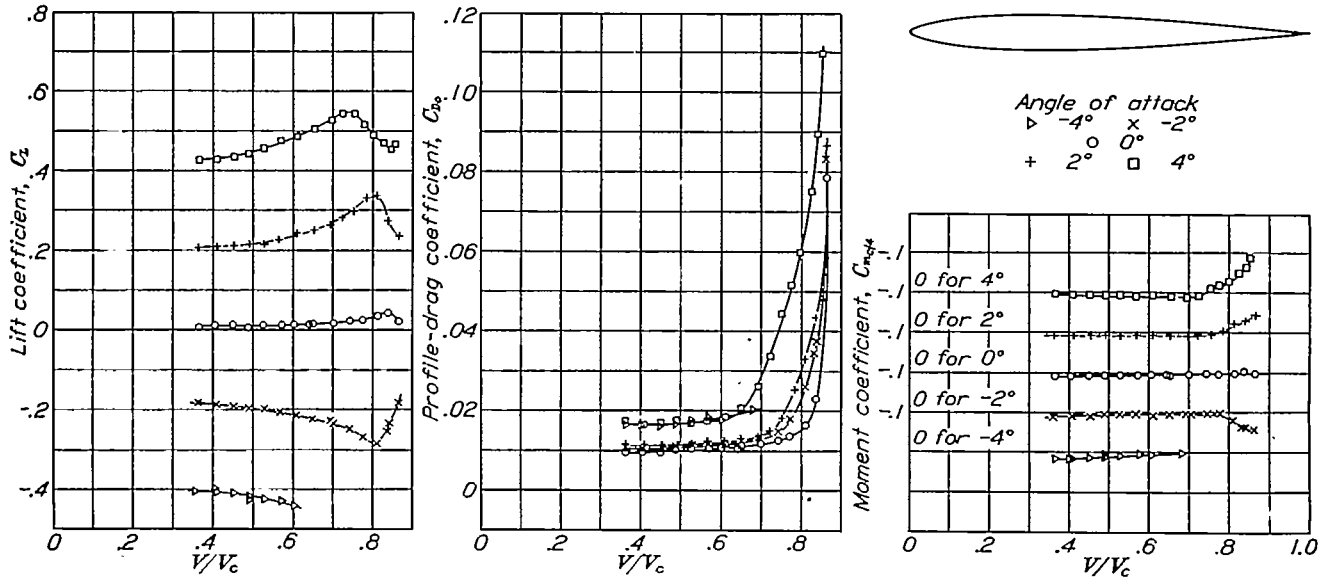

FIGURE 11.—Effect of compressibility on the aerodynamic characteristics of the N.A.C.A. 0009-33 airfoil.

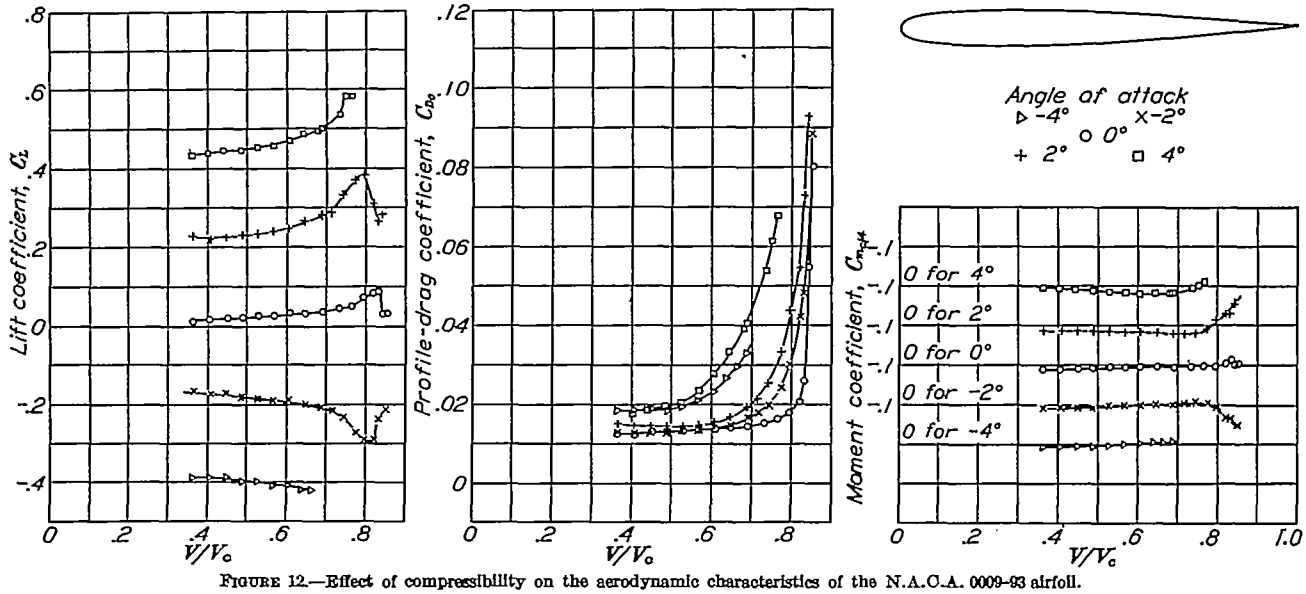

FIGURE 12.—Effect of compressibility on the aerodynamic characteristics of the N.A.C.A. 0009-93 airfoil.

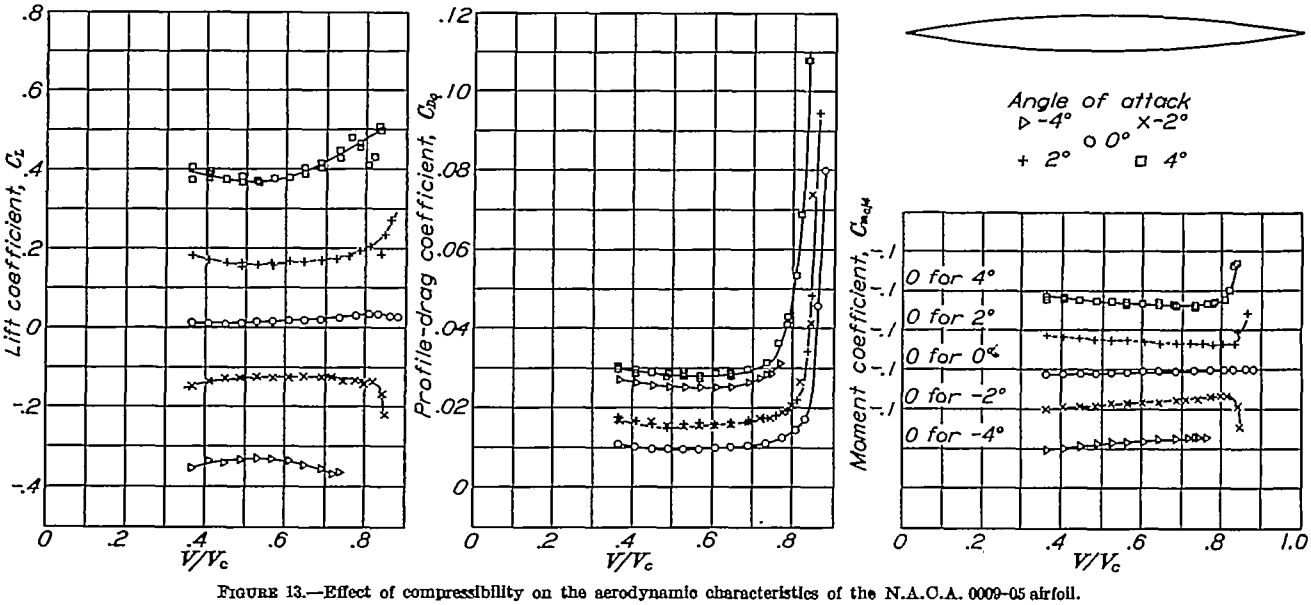

FIGURE 13.—Effect of compressibility on the aerodynamic characteristics of the N.A.C.A. 0009-05 airfoil.

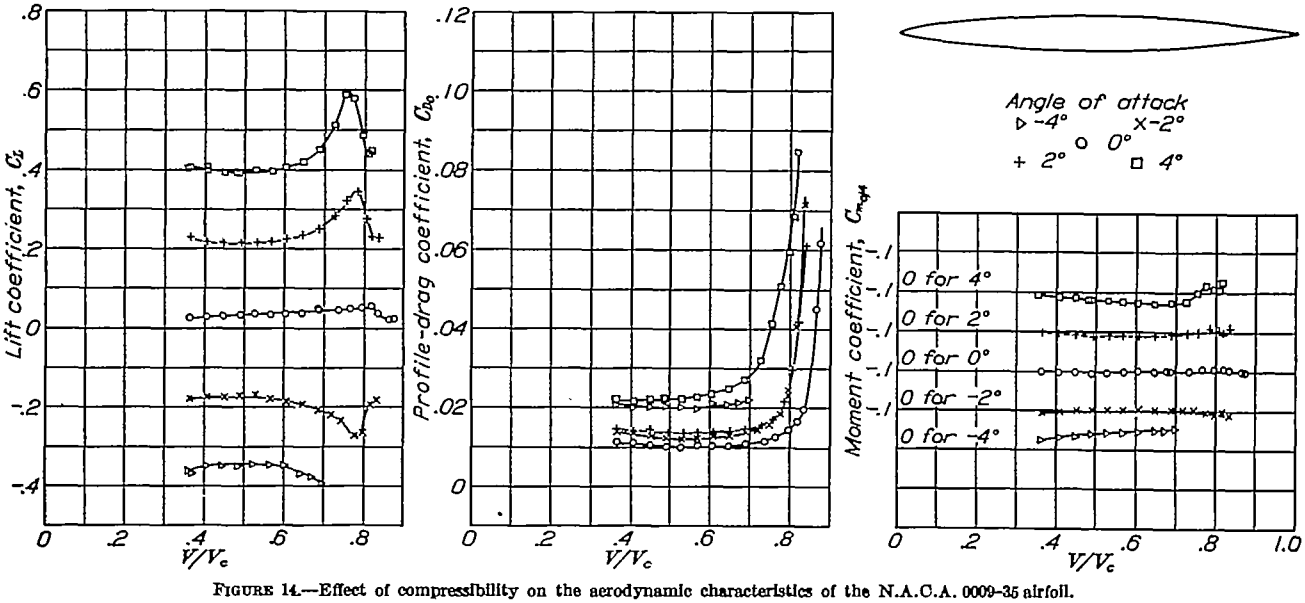

FIGURE 14.—Effect of compressibility on the aerodynamic characteristics of the N.A.C.A. 0009-35 airfoil.

to be used in developing better propeller sections. Because the Reynolds Number for the tests is somewhat lower than that at which most propellers operate, the data are not directly applicable to many propeller problems, but it is probable that some of the relations shown, particularly the relative effect of the shape changes as affected by compressibility, are valid at much higher values of the Reynolds Number.

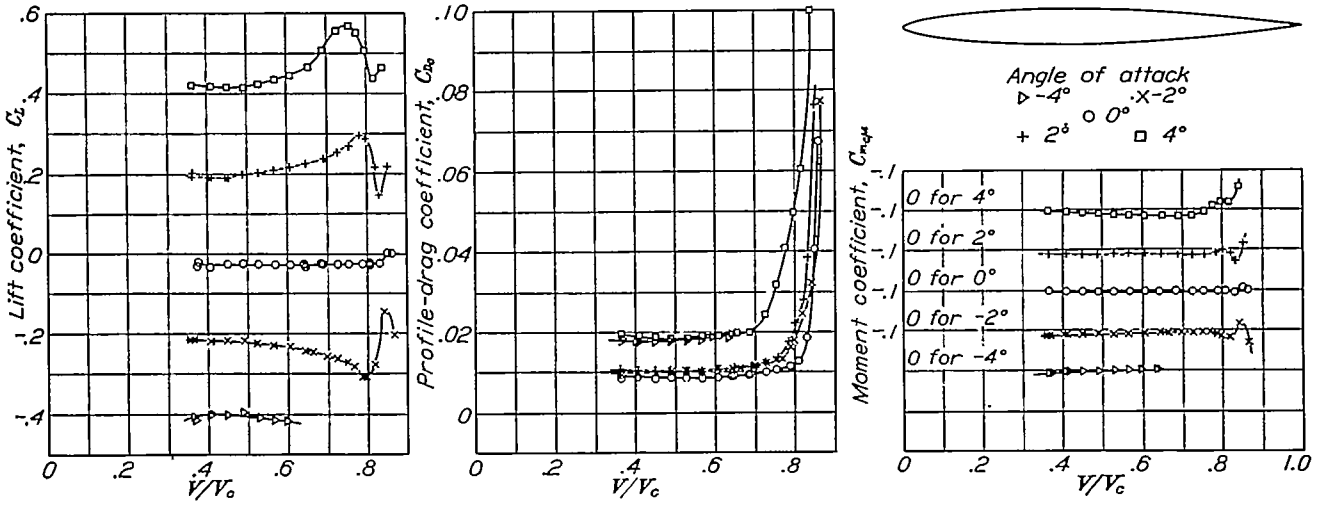

FIGURE 15.—Effect of compressibility on the aerodynamic characteristics of the N.A.C.A. 0009-34 airfoil.

PROFILE DRAG

The effects of compressibility on profile drag are substantially in agreement with the results shown in reference 1 and therefore are not discussed in detail. The changes in the drag coefficients are small until a speed corresponding to that of the compressibility burble is reached; the drag coefficient then rapidly increases.

Effect of thickness.—The effects of thickness on the minimum profile-drag coefficient and on the profile-drag coefficient for a lift coefficient of 0.4 are shown in figure 35. The minimum profile-drag coefficient increases uniformly with the thickness ratio of the airfoils at speeds below that of the compressibility burble. Increasing the thickness of an airfoil causes the compressibility burble to occur at progressively lower speeds. The profile-drag coefficients for a lift coefficient of 0.4 show, in general, the same changes as the minimum profile-drag coefficients, except for a slight decrease in the profile-drag coefficient with increase of speed over the lower end of the speed range. Figure 35 also shows that the speed at which the rapid rise in the drag coefficient or the compressibility burble occurs, decreases as the lift is increased.

Effect of maximum thickness position.—Curves showing the variation of the minimum profile-drag co-

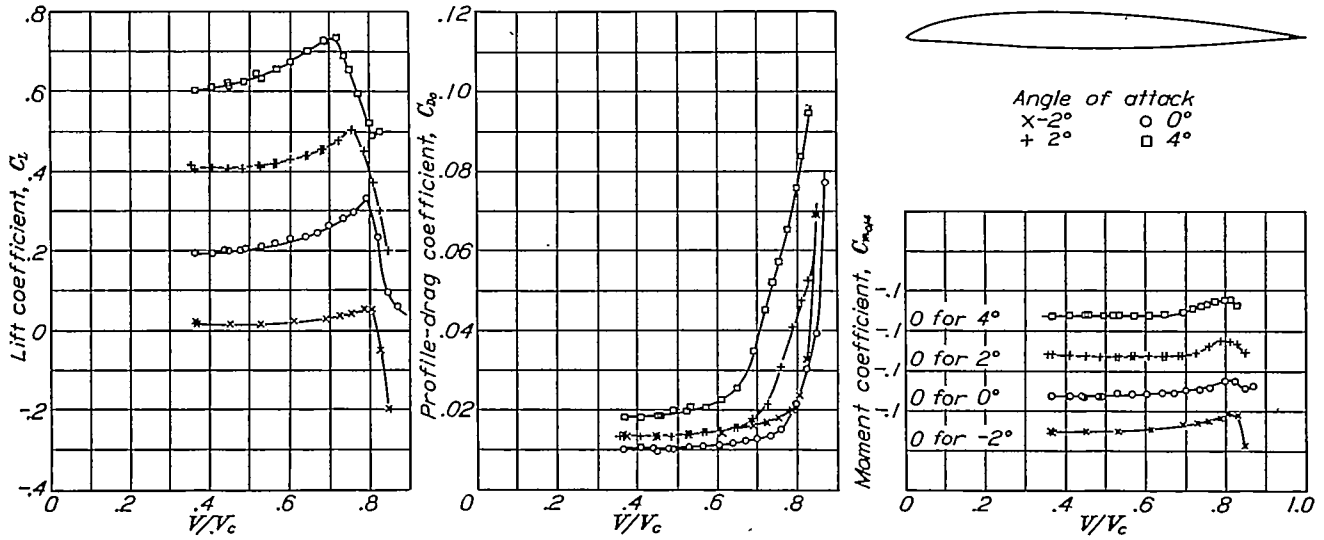

FIGURE 16.—Effect of compressibility on the aerodynamic characteristics of the N.A.C.A. 2209-34 airfoil.

efficient with speed, for airfoils having various positions of the maximum thickness, are given in figure 35. The N.A.C.A. 0009–64 has the lowest minimum profile drag over the entire speed range, and also has the highest speed for the compressibility burble. Airfoils having the position of maximum thickness forward or aft o the 40 percent location have progressively higher mini-

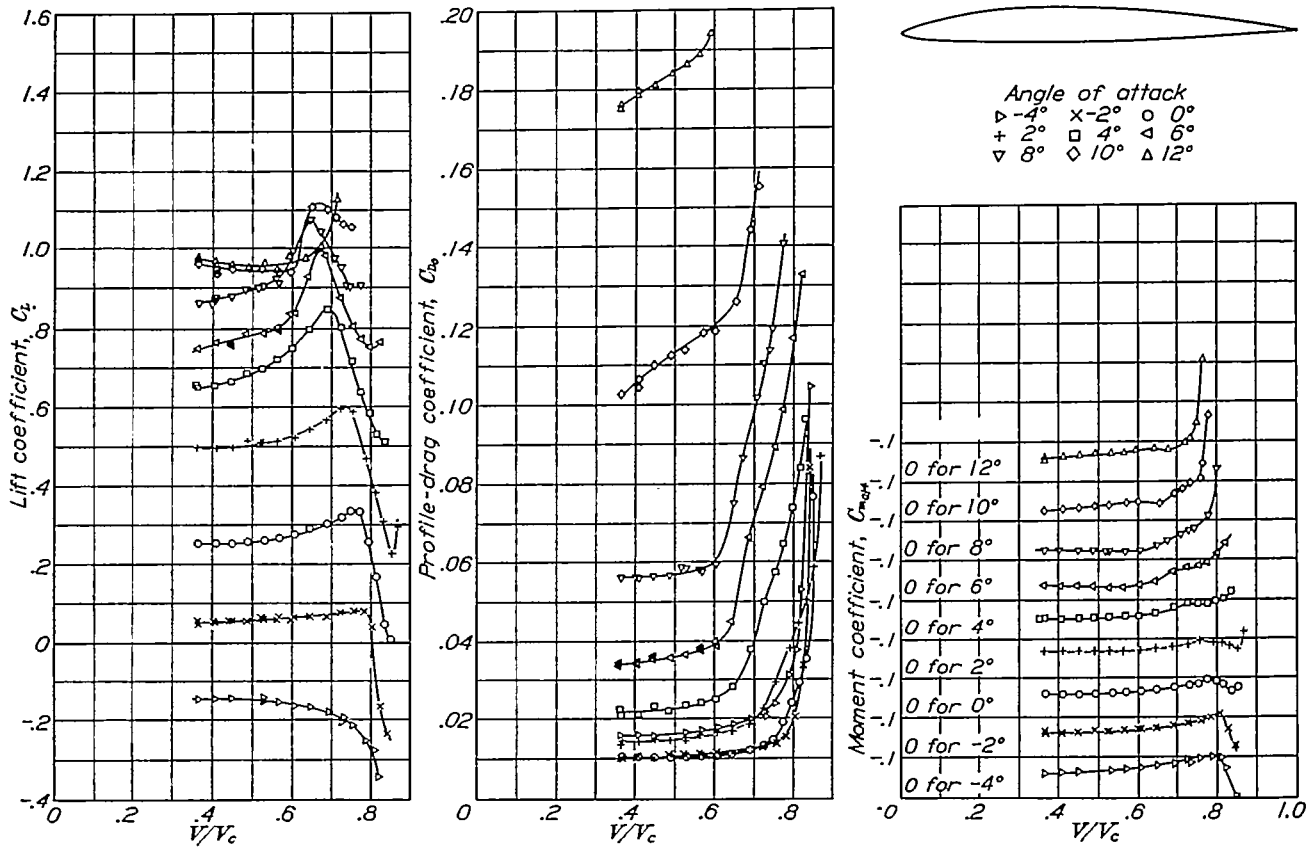

FIGURE 17.—Effect of compressibility on the aerodynamic characteristics of the N.A.C.A. 2409-34 airfoil.

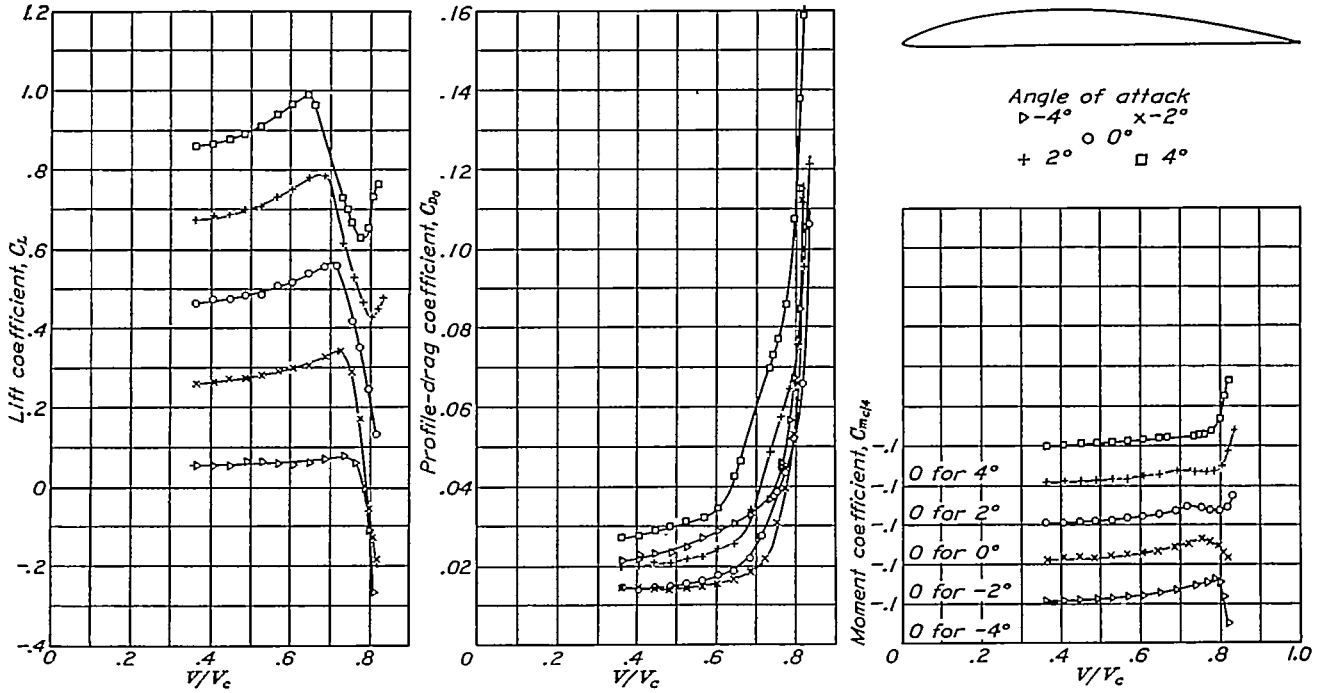

FIGURE 18.—Effect of compressibility on the aerodynamic characteristics of the N.A.C.A. 4409-34 airfoil.

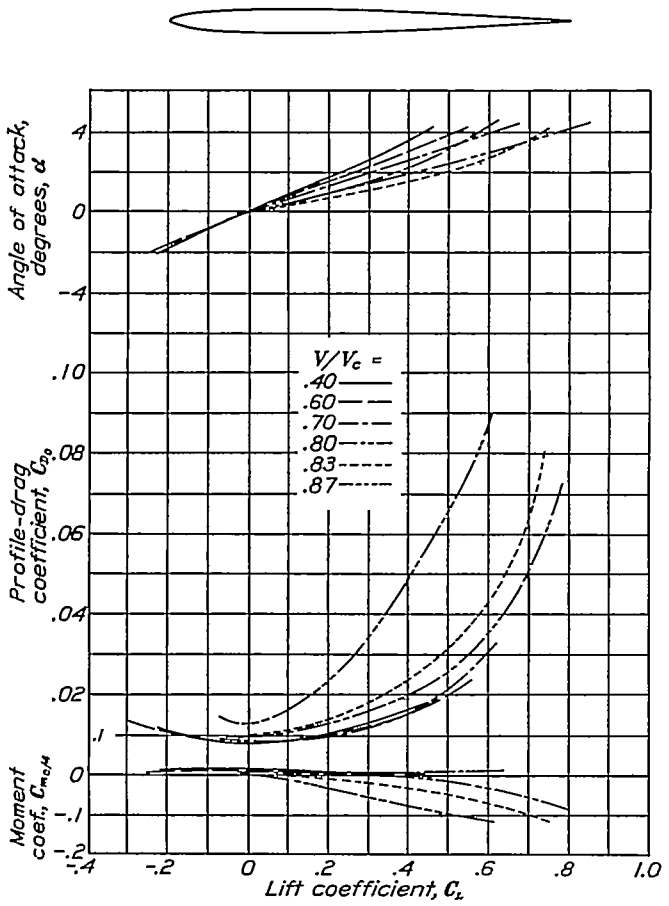

FIGURE 19.—Aerodynamic characteristics of the N.A.C.A. 0006-63 airfoil.

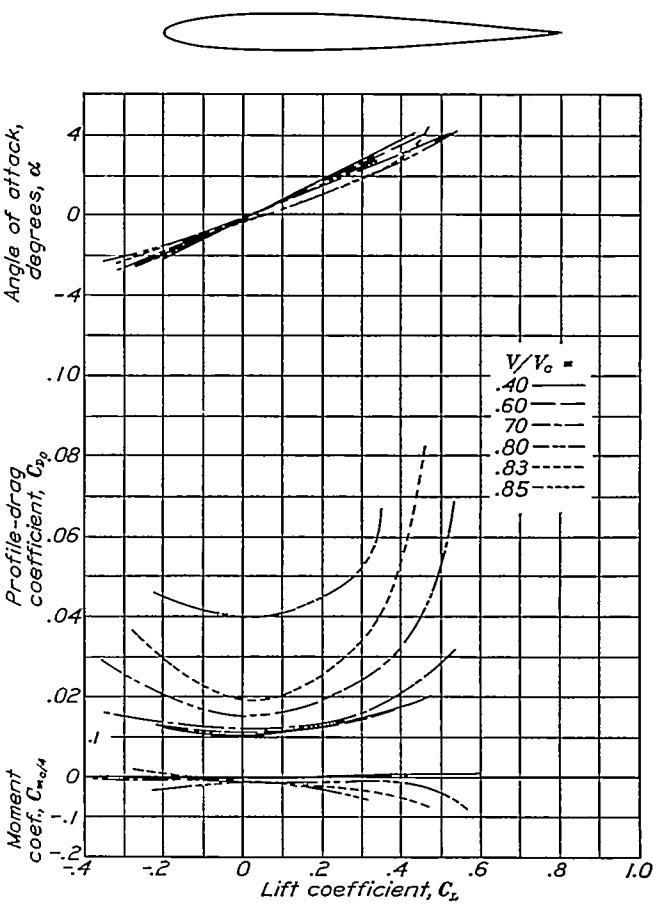

FIGURE 21.—Aerodynamic characteristics of the N.A.C.A. 0009-63 airfoil.

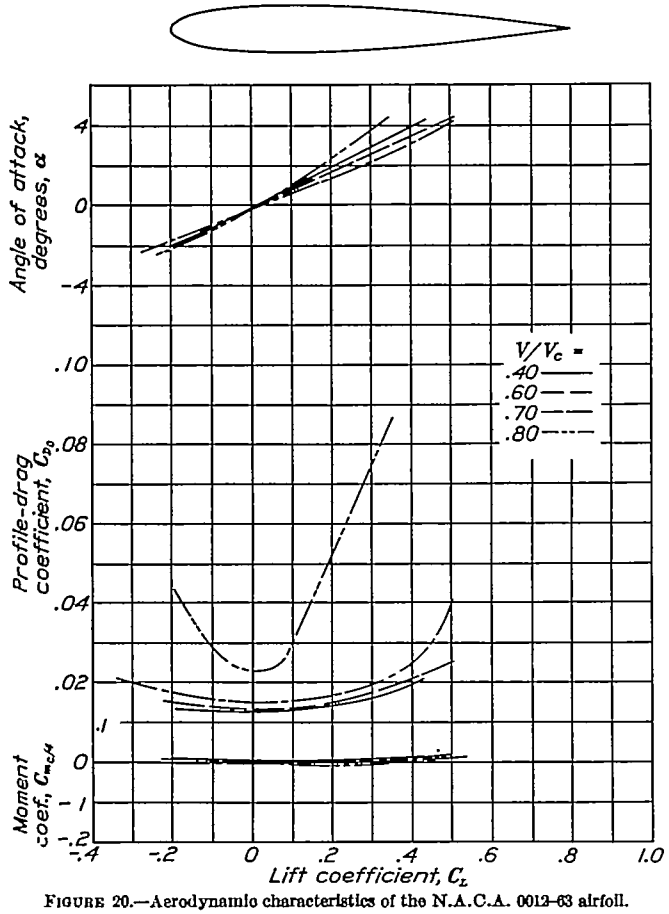

FIGURE 20.—Aerodynamic characteristics of the N.A.C.A. 0012-63 airfoil.

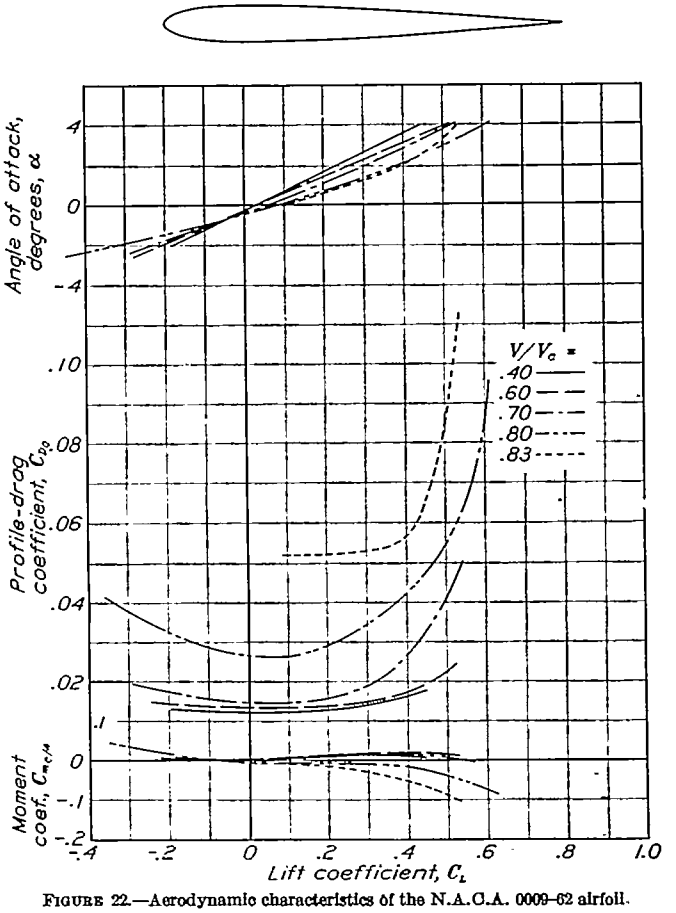

FIGURE 22.—Aerodynamic characteristics of the N.A.C.A. 0009-62 airfoil.

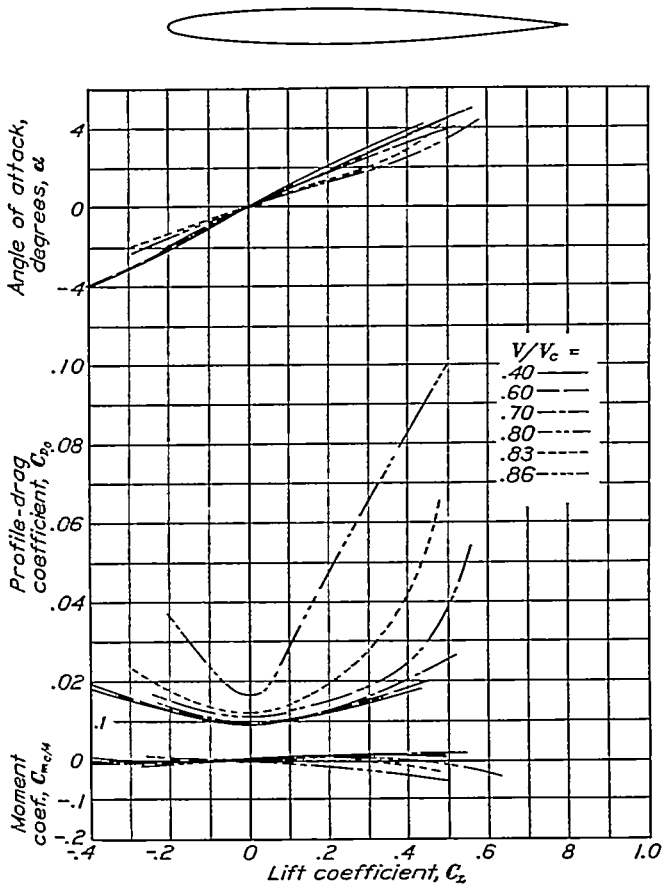

FIGURE 23.—Aerodynamic characteristics of the N.A.C.A. 0009-64 airfoil.

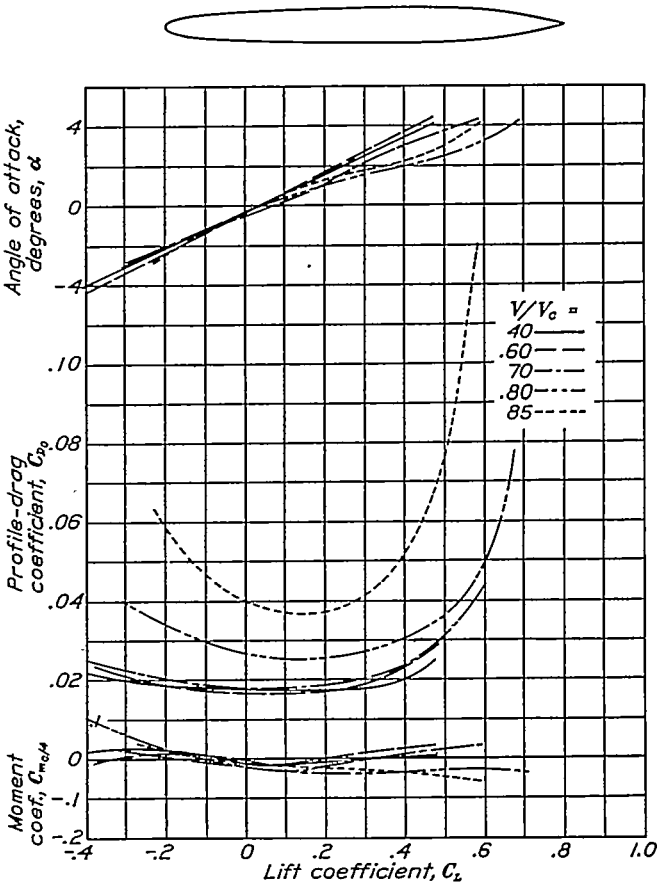

FIGURE 25.—Aerodynamic characteristics of the N.A.C.A. 0009-66 airfoil.

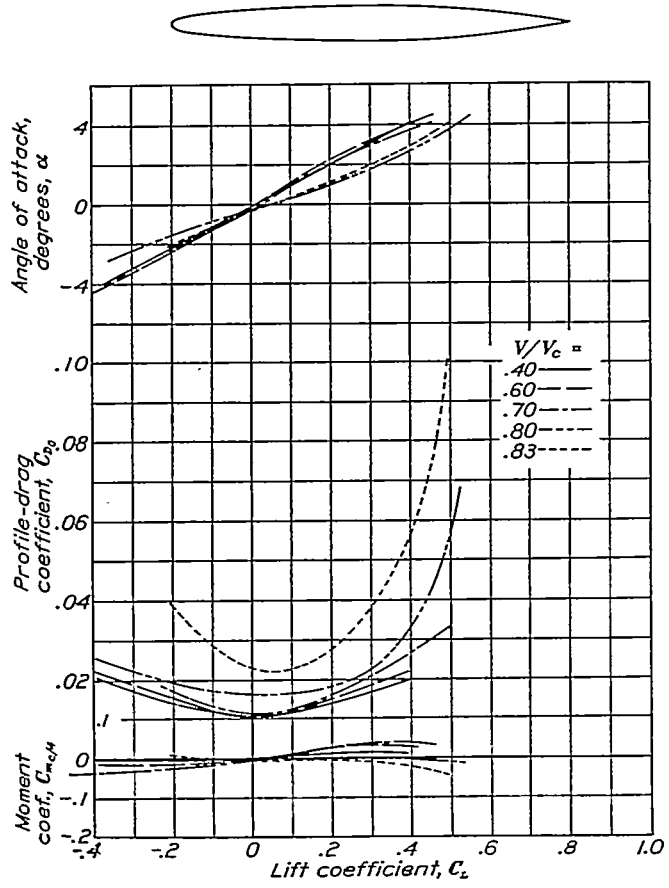

FIGURE 24.—Aerodynamic characteristics of the N.A.C.A. 0009-65 airfoil.

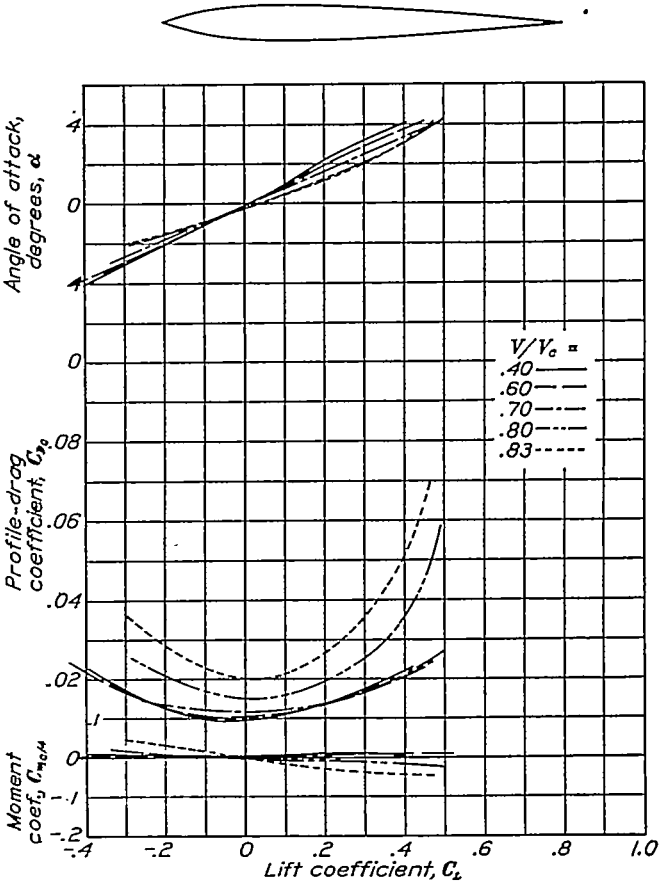

FIGURE 26.—Aerodynamic characteristics of the N.A.C.A. 0009-63 airfoil.

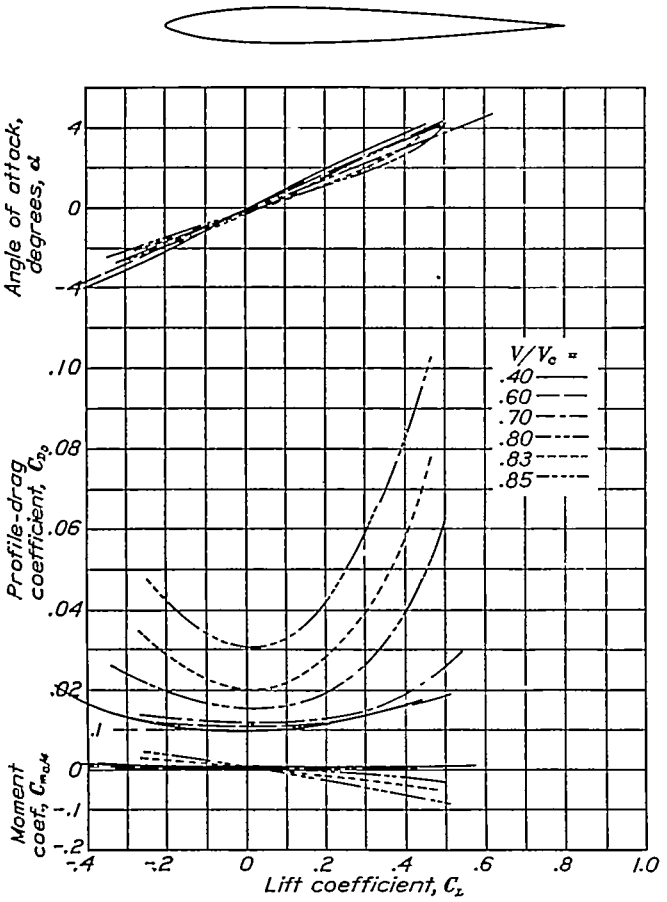

FIGURE 27.—Aerodynamic characteristics of the N.A.C.A. 0009-33 airfoil.

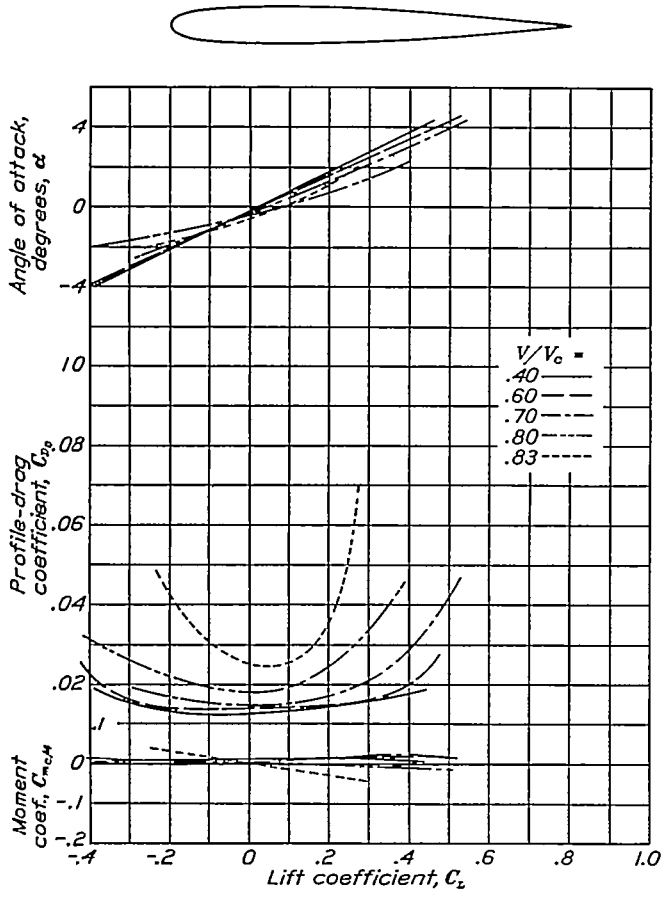

FIGURE 28.—Aerodynamic characteristics of the N.A.C.A. 0009-63 airfoil.

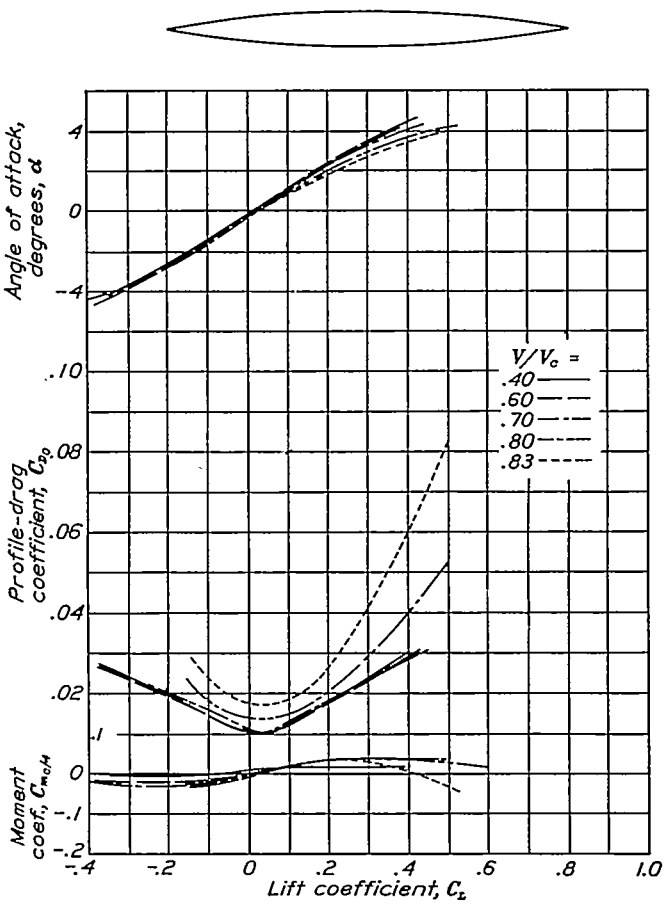

FIGURE 29.—Aerodynamic characteristics of the N.A.C.A. 0009-05 airfoil.

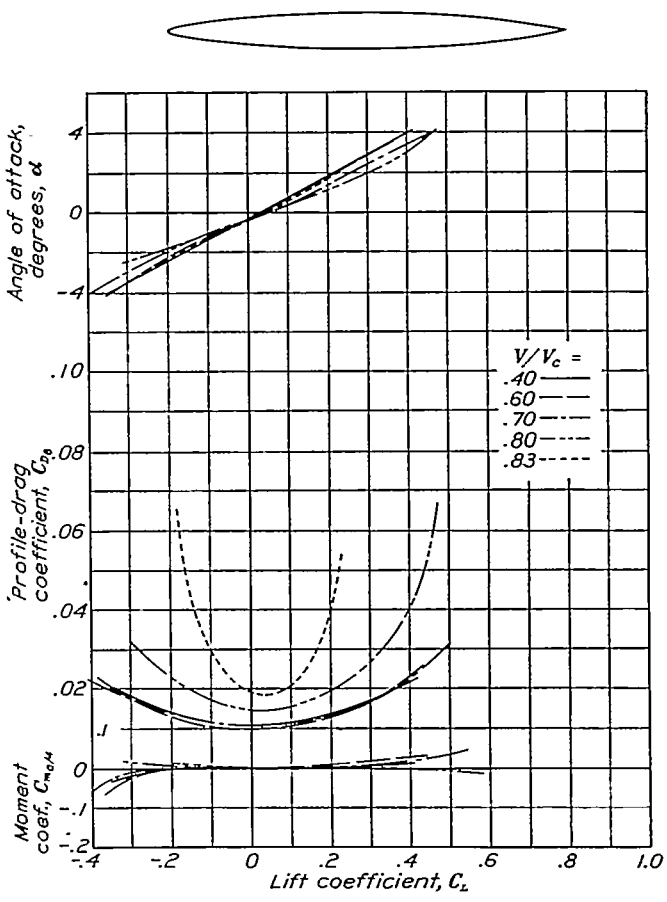

FIGURE 30.—Aerodynamic characteristics of the N.A.C.A. 0009-35 airfoil.

mum profile drags and earlier compressibility burbles.

Profile-drag coefficient curves for a lift coefficient of 0.4 are also shown in figure 35. Differences in the profile-drag coefficient between the 20, 30, and 40 percent locations are very small at the lower speeds. Airfoils having their maximum thicknesses located at 50 and 60 percent of the chord have the highest drag for speeds up to approximately 65 percent of the speed of sound. At higher speeds the airfoil having the farthest forward location of the maximum thickness becomes the poorest, due to the earlier compressibility burble. Considering the speed range as a whole, the 40 percent position seems to be the optimum.

Effect of leading-edge radius.—Figure 35 shows that the effects of changes in the leading-edge radius on minimum profile drag are negligible except for very

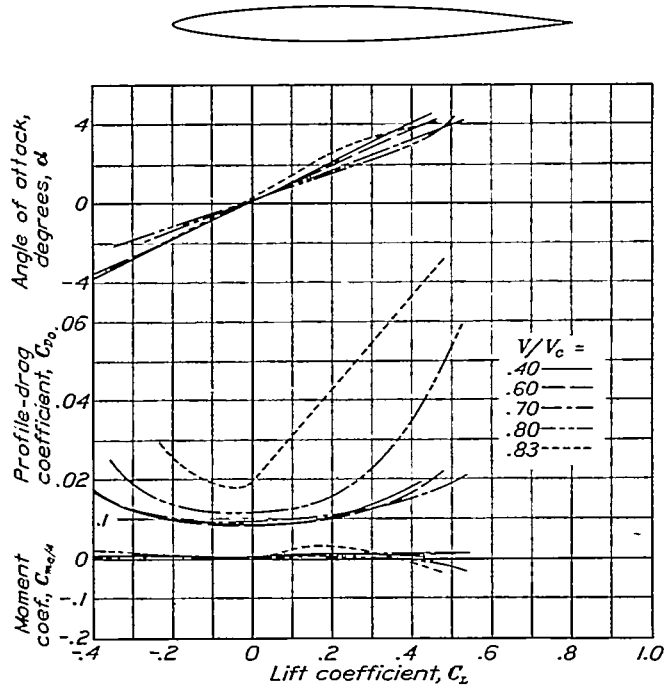

FIGURE 31.—Aerodynamic characteristics of the N.A.C.A. 0009-34 airfoil.

large values of the leading-edge radius. Airfoils having variations of the leading-edge radius from a sharp leading edge to the normal leading-edge radius have practically the same minimum profile drag over the entire speed range. An increase of the leading-edge radius to three times the normal value causes a relatively large increase in drag at the lower speeds, as well as an earlier compressibility burble.

With increase in lift, at lower speeds, the airfoil having a sharp leading edge has the highest profile drag due to the rapid drag increase with angle of attack. As the speed is increased the drag of the N.A.C.A. 0009–93 becomes greater, because of its earlier compressibility burble. The 0009–33 has the lowest profile drag. The quarter normal leading-edge radius is therefore the optimum value for the range of angle of attack tested.

Examination of the effects of variations of the leading-edge radius for airfoils having their maximum thickness located at 50 percent of the chord shows a slight increase in the minimum profile drag with increase of the leading-edge radius. At higher lift coefficients, there is a very large drag increase for the sharp leading edge. The airfoils having the leading-edge designations 3 and 6 show small differences.

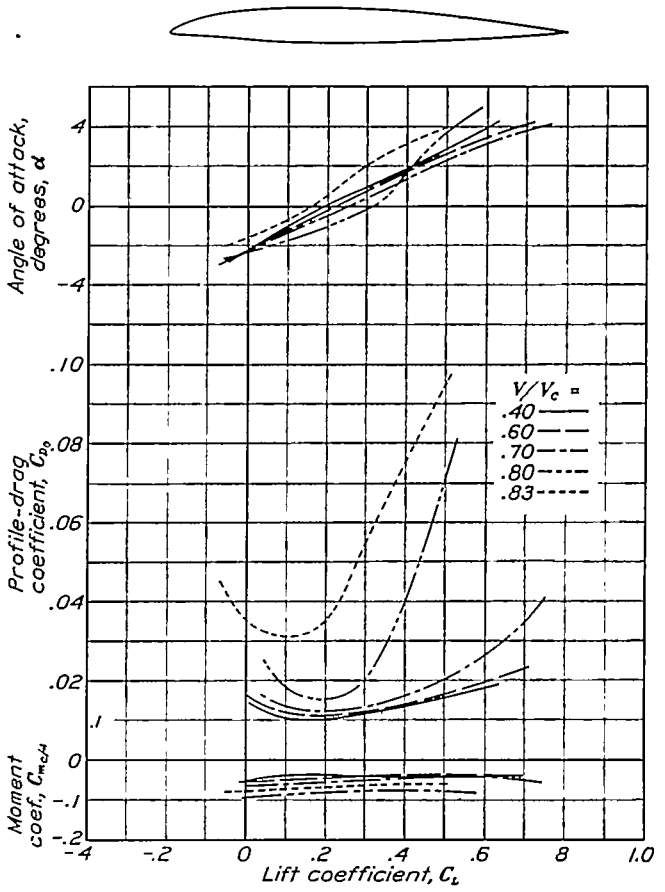

FIGURE 32.—Aerodynamic characteristics of the N.A.C.A. 2209-34 airfoil.

LIFT

The lift coefficients for symmetrical airfoils in the usual working range can be expressed in the following manner:

$$C_L = \frac{dC_L}{d\alpha}\alpha$$

where $\frac{dC_L}{d\alpha}$ (the lift-curve slope) depends on the shape of the airfoil and the flow parameters. For speeds below that of the compressibility burble it has been shown theoretically in references 4 and 5 that, as a first approximation, the effect of compressibility on lift is to increase $\frac{dC_L}{d\alpha}$ with the factor $\frac{1}{\sqrt{1-\left(\frac{V}{V_c}\right)^2}}$. This factor has been substantiated experimentally for speeds below that at which the compressibility burble

occurs, as shown in reference 1 and by figures 36, 37, and 38 of this report. At speeds in excess of that at which the compressibility burble occurs the value of $\frac{dC_L}{d\alpha}$ decreases very rapidly.

Effect of thickness.—The effect of increasing thickness on $\frac{dC_L}{d\alpha}$ is shown in figure 36. The lift-curve slope $\frac{dC_L}{d\alpha}$, in general, decreases with increase of thickness, a result in agreement with previous low-speed tests. Figure 36 also shows that the speeds at which $\frac{dC_L}{d\alpha}$ attains its maximum value decrease progressively with increasing thickness. The earlier compressibility burble for thicker airfoils shows clearly that the useful speed range decreases as the airfoil thickness increases.

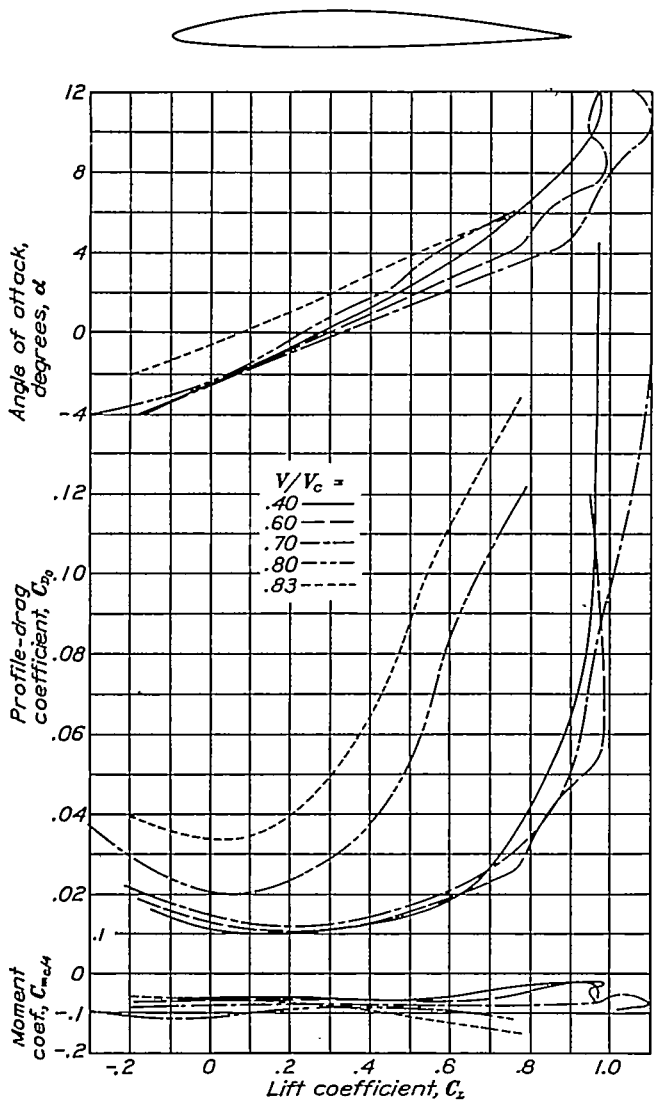

FIGURE 33.—Aerodynamic characteristics of the N.A.C.A. 2409-34 airfoil.

Effect of maximum thickness position.—The effects of variation in the maximum-thickness position on $\frac{dC_L}{d\alpha}$ are shown in figure 37. All the airfoils in this group have the normal leading-edge radius and a maximum thickness ratio t/c of 0.09. At the lower speeds, it is apparent that the value of $\frac{dC_L}{d\alpha}$ decreases almost uniformly with rearward movement of the maximum thickness until the maximum thickness is located approximately at mid chord. Additional rearward movement tends to increase the value of $\frac{dC_L}{d\alpha}$ slightly. As the speeds are increased the airfoils having extreme rear locations of the maximum thickness are inferior because of an earlier compressibility burble (fig. 37). Movement of the maximum thickness forward of the 30 percent location tends to increase the magnitude of the compressibility effect as is shown by the rapid rise at high speeds in the $\frac{dC_L}{d\alpha}$ curve for the 0009–62 airfoil. The later compressibility burble shown by the 0009–63 and 0009–64 airfoils indicates that the airfoils having the widest useful speed range will have their maximum thickness located between 30 to 40 percent of the chord aft of the leading edge.

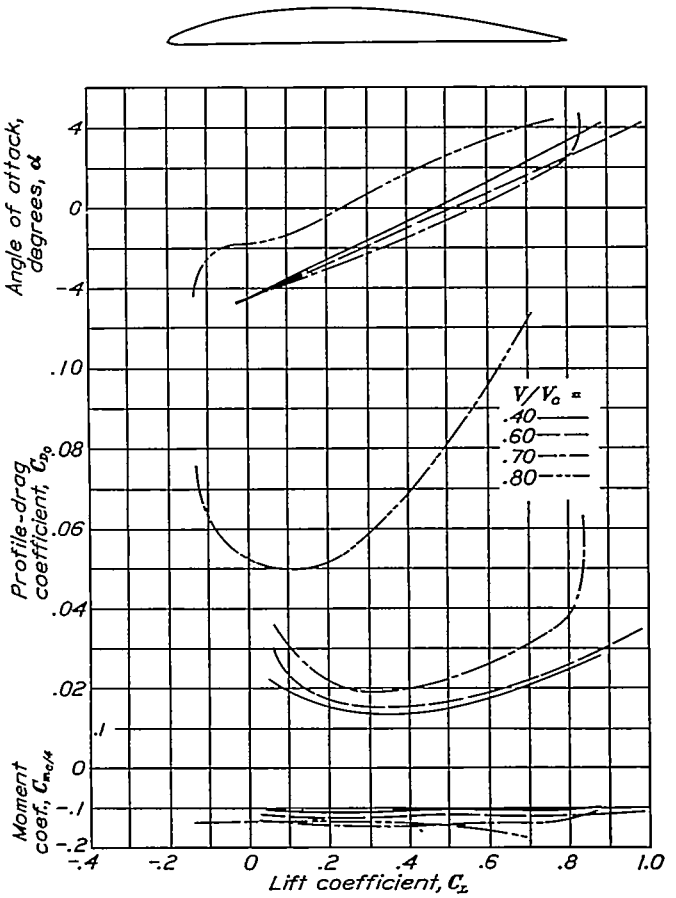

FIGURE 34.—Aerodynamic characteristics of the N.A.C.A. 4409-34 airfoil.

Effect of leading-edge radius.—The effects of variations in the leading-edge radius on the lift-curve slope for airfoils having the maximum thickness located at 30 percent of the chord and also at 50 percent of the chord aft of the leading edge are shown in figure 38.

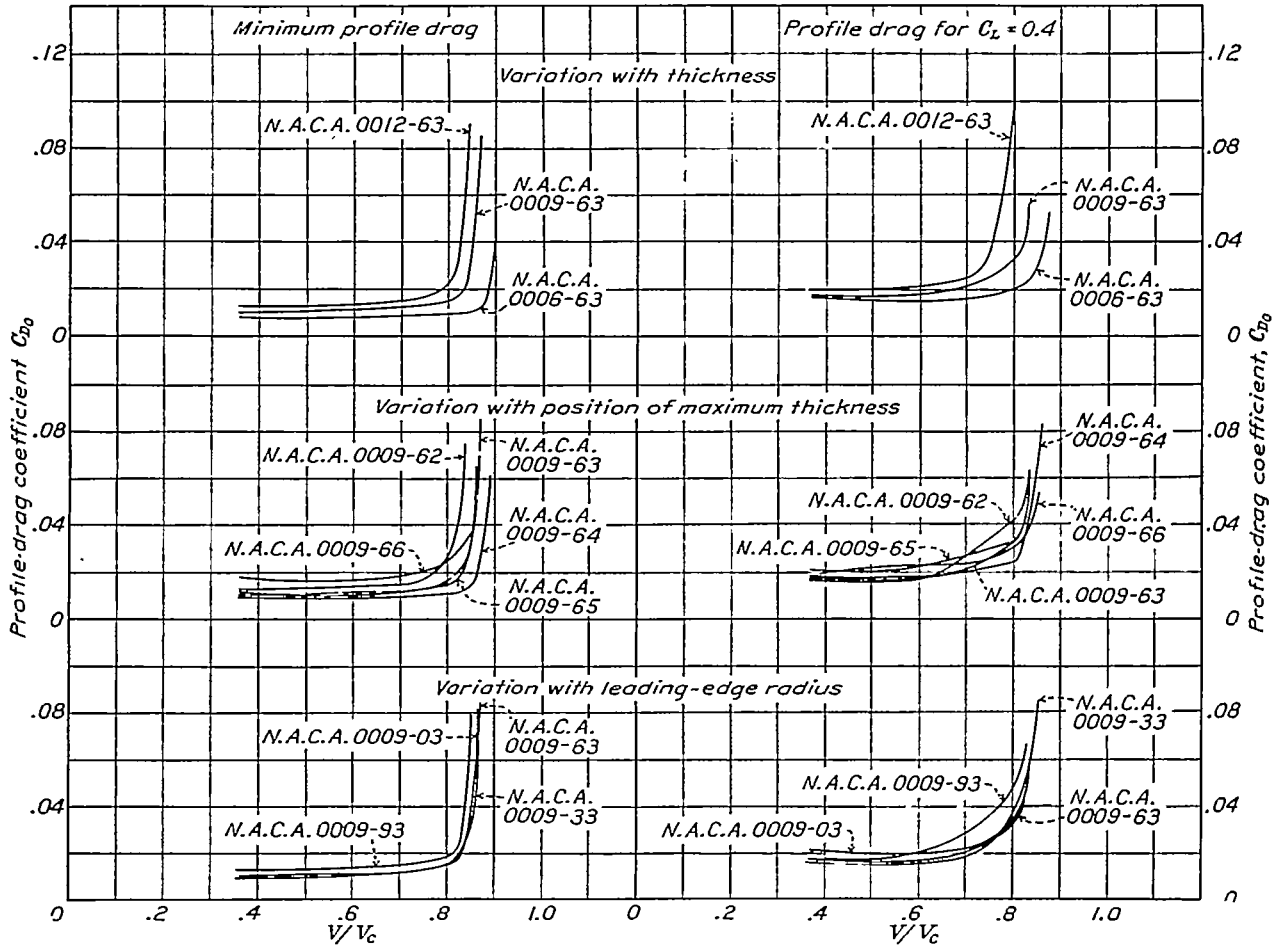

FIGURE 35.—Effect of compressibility on profile drag.

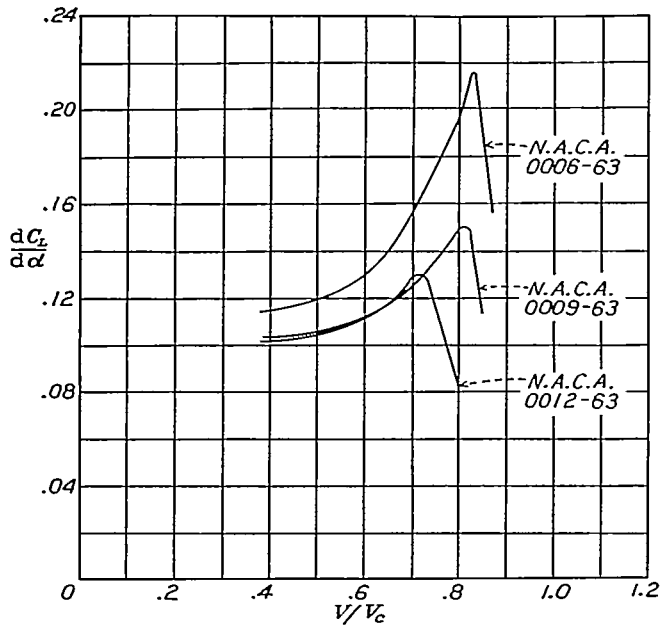

FIGURE 36.—Effect of compressibility on lift-curve slope. Variation with thickness.

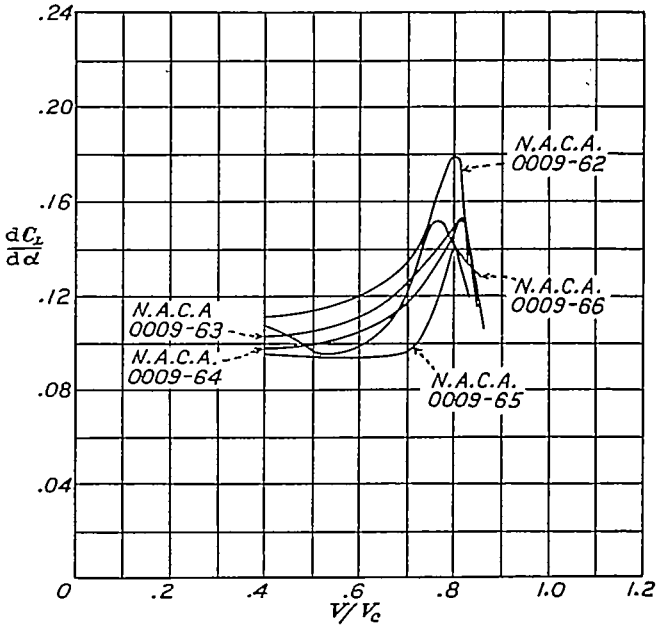

FIGURE 37.—Effect of compressibility on lift-curve slope. Variation with position of maximum thickness.

Considering first the airfoils having the maximum thickness located at 30 percent of the chord, it is apparent that the sharp leading edge is definitely bad. Variations of the leading-edge radius, provided that the leading edge is rounded, have apparently negligible effect on $\frac{dC_L}{d\alpha}$ at lower speeds, in agreement with the results of reference 2. It is to be noted that the blunt-nosed airfoil, the N.A.C.A. 0009–93, shows a very rapid rise in $\frac{dC_L}{d\alpha}$ at high speeds. This rapid rise in $\frac{dC_L}{d\alpha}$ is also shown by the 0009–62 airfoil, which has its maximum thickness well forward. It should also be noted that the compressibility burble tends to occur progressively at lower speeds as the leading-edge radius is increased.

Similiarity of the effects of increasing leading-edge radius to the effects of increasing thickness might have been expected because of the higher induced velocities over the forward portion of the airfoil caused by such form changes. Results of the tests of airfoils with various leading-edge radii having their maximum thickness located at 50 percent of the chord are in substantial agreement with the results obtained from the tests with the airfoils having their maximum thickness located at 30 percent of the chord, except that the compressibility burble shown by the airfoil having the normal leading-edge radius occurs at the higher speed.

TESTS OF CAMBERED AIRFOILS

A detailed study of camber variations has not been attempted as part of this investigation. However, in order to study the application of the data obtained from the symmetrical airfoil tests as well as to develop, if possible, by means of a few tests, a more efficient practical propeller section and to indicate the general trend of the effects of camber particularly at high speeds, a few airfoils having certain camber variations and one of the best thickness forms have been tested.

Selection of thickness form.—The choice of the best form for the thickness distribution was made principally on the basis of low drag and late compressibility burble. Within the lift-coefficient range investigated, the tests of symmetrical airfoils indicate that, for an airfoil of medium thickness, the maximum thickness should be located at 40 percent of the chord aft of the leading edge and the leading-edge radius should be one-quarter of the normal value. Thus, the 34-thickness distribution would seem to be the best. The N.A.C.A. 0009–34 and three cambered airfoils having this thickness distribution were therefore built and tested. A comparison of the N.A.C.A. 0009–64 and N.A.C.A. 0009–34 airfoils (figs. 23 and 31) shows that, except for the slightly earlier compressibility burble of the N.A.C.A. 0009–34 airfoil, there is practically no difference in the minimum profile drag of these airfoils. At moderate lift coefficients the profile drag of the N.A.C.A. 0009–34 decreases slightly with increasing speed, whereas the profile drag of the N.A.C.A. 0009–64 increases. Because of this difference, which may be attributed to the more gradual compressibility burble of the N.A.C.A. 0009–64, the N.A.C.A. 0009–34 has a lower profile drag over part of the speed range. As at minimum drag, however, the N.A.C.A. 0009–34 has the earlier compressibility burble. From this comparison it is apparent that the general superiority of either of these airfoils is difficult to establish. This comparison shows, however, that the shift of the maximum ordinate from the normal to the 40 percent location causes much greater improvement than can be obtained from small changes in the leading-edge radius. Future tests to study camber effects should probably

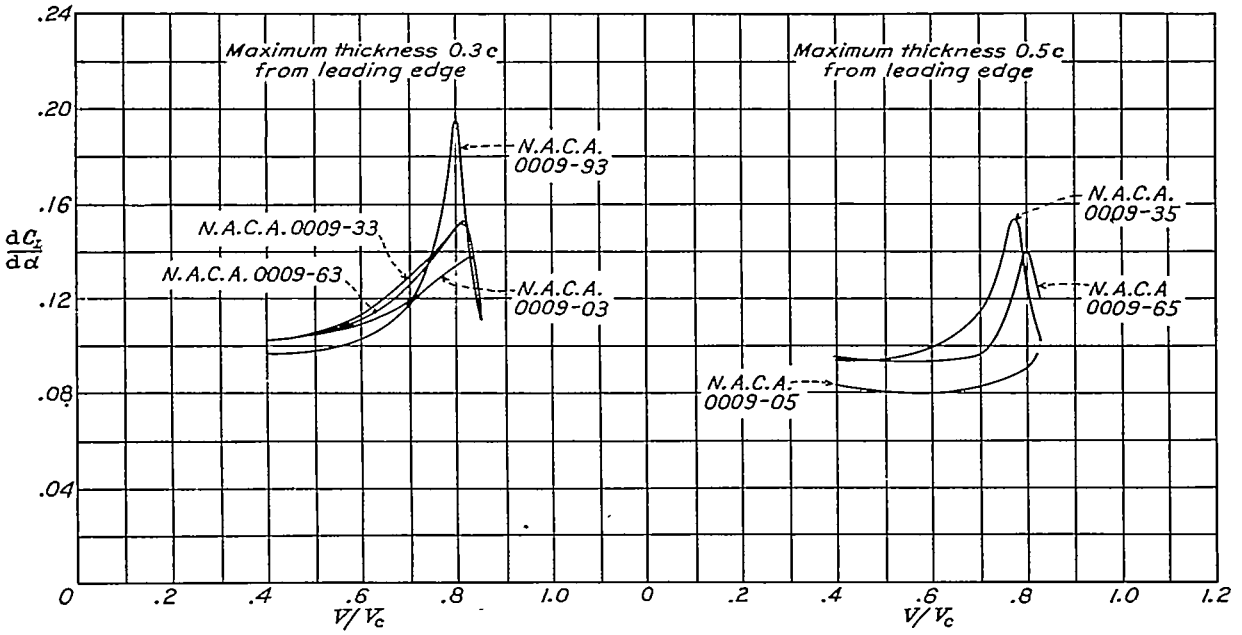

FIGURE 38.—Effect of compressibility on lift-curve slope. Variation with leading-edge radius.

include some tests of airfoils having both thickness forms.

Camber form.—Tests of the cambered airfoils were first conducted at low angles of attack. The best of these airfoils on the basis of low profile drag and late compressibility burble was then chosen for testing at high angles of attack.

drag. At high speeds, the N.A.C.A. 2409–34 becomes superior to both the other airfoils except for a narrow range of lift coefficients within which the N.A.C.A. 2209–34 has a smaller profile drag.

The results given in figures 31 to 34 showing the effects of changes in the mean line on the aerodynamic characteristics are in general agreement with previous

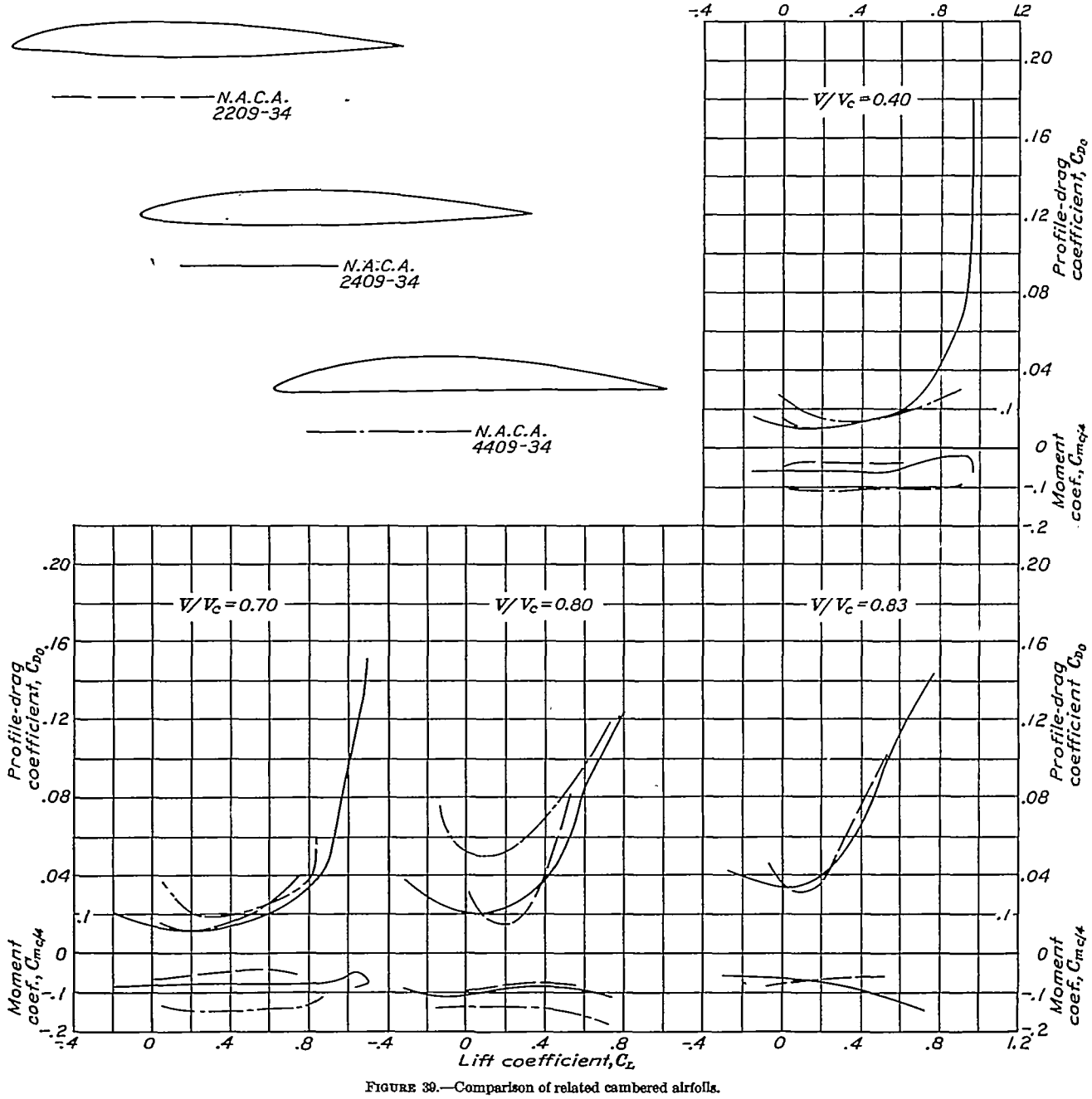

FIGURE 39.—Comparison of related cambered airfoils.

Figure 39 gives a comparison of the three cambered airfoils tested, the N.A.C.A. 2209–34, N.A.C.A. 2409–34, and the N.A.C.A. 4409–34. At low speeds the N.A.C.A. 2409–34 has the lowest minimum profile drag. The data thus far obtained indicate that the N.A.C.A. 4409–34 has the highest maximum lift coefficient, but it has also the highest minimum profile

investigations at low speeds. The changes in the moment coefficient and in the angle of zero lift at low speed are due principally to changes in the mean line, and are qualitatively in accord with thin-airfoil theory. At high speeds larger differences are apparent. These differences are due to the effects of camber changes on the speed at which the compressibility burble occurs.

Effects of compressibility.—The effects of compressibility on the lift and drag of the cambered airfoils are similar to those previously discussed for the symmetrical airfoils. Some compressibility effects occur on cambered airfoils that are not shown by the symmetrical airfoils. As the speed corresponding to the compressibility burble is exceeded, the angle of zero lift α_{L_0} suddenly tends toward zero. An effective displacement of the lift curve occurs.

Over the lower portion of the speed range the negative moment coefficient increases with increase of speed. The relative amount of the increase is approximately the same as the increase in the lift coefficient. The location of the center of pressure, therefore, remains practically constant. When the speed is increased above that at which the compressibility burble occurs, the lift coefficient decreases rapidly and the negative moment coefficient increases rapidly; consequently, there is a large and rapid rearward movement of the center of pressure. The magnitude of the change in the moment coefficient over the low-speed part of the range is sufficiently large to warrant full-scale studies to obtain information for the design of wings for diving bombers.

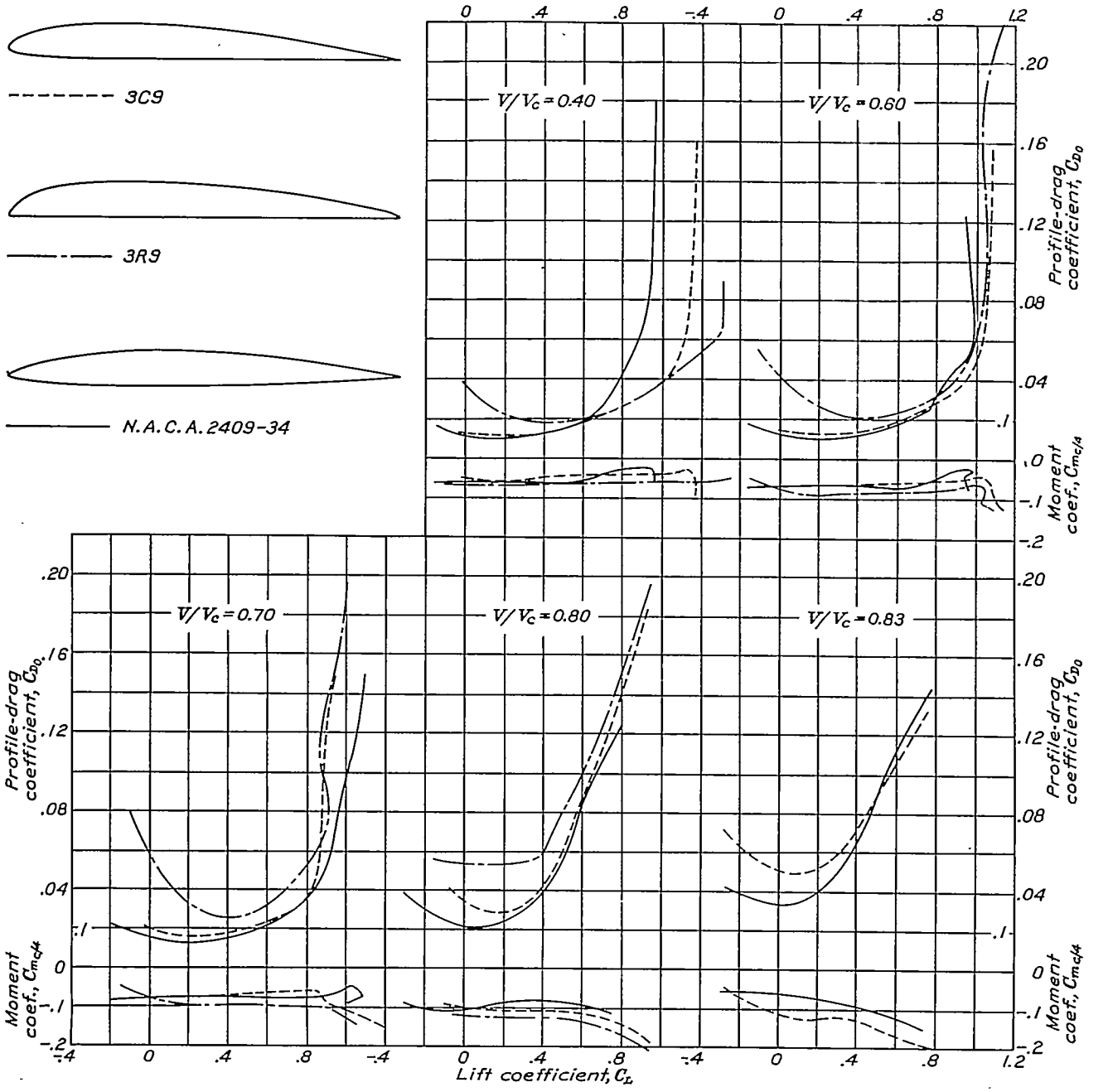

FIGURE 40.—Comparison of 3C9, 3R9, and N.A.C.A. 2409-34 airfoils.

Comparison of cambered airfoils.—A comparison of the N.A.C.A. 2409–34 airfoil with the 3C9 and 3R9 airfoils is given in figure 40. The data for the 3C9 and 3R9 have been interpolated from the results presented

in reference 1. At the lower speeds the N.A.C.A. 2409–34 has the lowest minimum drag, the lowest maximum lift, and therefore the smallest useful angular range. As the speed is increased above six-tenths of the speed of sound the N.A.C.A. 2409–34 airfoil becomes superior to both the 3C9 and the 3R9 airfoils, because of the larger compressibility effect on the C and R airfoils.

It is probable that the low-speed maximum lift of the N.A.C.A. 2409–34 could be increased by increasing the leading-edge radius. Because the effect of the leading-edge radius on profile drag is small, it would seem that the 2409–64 airfoil section might be better for applications requiring a section to operate over a considerable range of the lift coefficient. In the development of cambered airfoils, of which the three tested form a preliminary step, the effects of shape variations on the maximum lift will be more thoroughly investigated, particularly at the lower speeds.

CONCLUSIONS

The principal factors affecting the choice of propeller sections are low drag at low and moderate lift coefficients and a late compressibility burble; that is, low drags at high speeds. Considering these factors, these results indicate:

1. The airfoil thickness should be small.
2. The best position for the maximum thickness is approximately 40 percent of the chord aft of the leading edge.
3. The optimum values of the leading-edge radius lie between 0.22 percent and 0.89 percent of the chord for airfoils of 9 percent thickness.
4. At high speeds the N.A.C.A. 2409–34 airfoil is superior to the commonly used propeller sections. The results indicate that some further improvement may be expected.

LANGLEY MEMORIAL AERONAUTICAL LABORATORY,
NATIONAL ADVISORY COMMITTEE FOR AERONAUTICS,
LANGLEY FIELD, VA., *April 28, 1934.*

REFERENCES

1. Stack, John: The N.A.C.A. High-Speed Wind Tunnel and Tests of Six Propeller Sections. T.R. No. 463, N.A.C.A., 1933.
2. Jacobs, Eastman N., Ward, Kenneth E., and Pinkerton, Robert M.: The Characteristics of 78 Related Airfoil Sections from Tests in the Variable-Density Wind Tunnel. T.R. No. 460, N.A.C.A., 1933.
3. Jacobs, Eastman N., and Abbott, Ira H.: The N.A.C.A. Variable-Density Wind Tunnel. T.R. No. 416, N.A.C.A., 1932.
4. Ackeret, J.: Über Luftkräfte bei sehr grossen Geschwindigkeiten insbesondere bei ebenen Strömungen. Helvetica Physica Acta, vol. I, Fasciculus Quintus, 1928, pp. 301–322.
5. Glauert, H.: The Effect of Compressibility on the Lift of an Aerofoil. R. & M. No. 1135, British A.R.C., 1928.

TABLE I

ORDINATES OF AIRFOILS

Station \ Airfoil	0006-63	0012-63	0009-63	0009-62	0009-64	0009-65	0009-66	0009-03	0009-33	0009-93	0009-05	0009-35	0009-34	2209-34		2409-34		4409-34	
														Upper surface	Lower surface	Upper surface	Lower surface	Upper surface	Lower surface
0	0	0	0	0	0	0	0	0	0	0	0	0	0		0		0		0
0.0125	0.0096	0.0191	0.0144	0.0159	0.0136	0.0132	0.0134	0.0050	0.0097	0.0212	0.0026	0.0079	0.0085	0.0117	−0.0059	0.0100	−0.0070	0.0117	−0.0054
.0250	.0133	.0265	.0199	.0227	.0184	.0177	.0181	.0096	.0147	.0274	.0052	.0114	.0126	.0180	−.0073	.0153	−.0100	.0183	−.0073
.0500	.0181	.0362	.0271	.0317	.0245	.0233	.0239	.0177	.0224	.0340	.0100	.0166	.0187	.0281	−.0094	.0239	−.0137	.0290	−.0090
.0750	.0214	.0428	.0321	.0374	.0286	.0269	.0278	.0245	.0283	.0376	.0144	.0206	.0235	.0364	−.0109	.0308	−.0163	.0380	−.0095
.1000	.0238	.0476	.0357	.0410	.0318	.0297	.0306	.0301	.0329	.0399	.0184	.0240	.0274	.0430	−.0122	.0367	−.0183	.0458	−.0090
.1500	.0271	.0541	.0406	.0444	.0365	.0338	.0347	.0380	.0393	.0425	.0255	.0296	.0337	.0527	−.0147	.0461	−.0212	.0580	−.0090
.2000	.0289	.0579	.0433	.0450	.0397	.0368	.0376	.0425	.0429	.0439	.0313	.0341	.0382	.0582	−.0182	.0534	−.0231	.0685	−.0081
.3000	.0300	.0600	.0450	.0441	.0437	.0412	.0412	.0450	.0450	.0450	.0395	.0403	.0435	.0632	−.0238	.0623	−.0247	.0811	−.0060
.4000	.0292	.0585	.0438	.0415	.0450	.0440	.0434	.0438	.0438	.0438	.0438	.0439	.0450	.0638	−.0262	.0650	−.0250	.0850	−.0050
.5000	.0270	.0541	.0406	.0374	.0437	.0450	.0446	.0406	.0403	.0406	.0450	.0450	.0437	.0610	−.0265	.0632	−.0242	.0827	−.0048
.6000	.0236	.0472	.0354	.0320	.0399	.0438	.0450	.0354	.0354	.0354	.0438	.0438	.0399	.0550	−.0249	.0577	−.0221	.0750	−.0043
.7000	.0190	.0381	.0286	.0254	.0336	.0395	.0440	.0286	.0286	.0286	.0395	.0395	.0336	.0460	−.0213	.0487	−.0185	.0640	−.0035
.8000	.0136	.0272	.0204	.0179	.0249	.0315	.0387	.0204	.0204	.0204	.0315	.0315	.0249	.0338	−.0161	.0363	−.0137	.0477	−.0020
.9000	.0074	.0148	.0111	.0096	.0140	.0189	.0255	.0111	.0111	.0111	.0189	.0189	.0140	.0188	−.0092	.0203	−.0078	.0267	−.0018
.9500	.0041	.0081	.0061	.0054	.0077	.0106	.0149	.0061	.0061	.0061	.0106	.0106	.0077	.0102	−.0052	.0109	−.0044	.0141	−.0014
1.0000	.0006	.0012	.0009	.0009	.0009	.0009	.0009	.0009	.0009	.0009	.0009	.0009	.0009	.0009	−.0009	.0009	−.0009	.0009	−.0009
Leading-edge radius	.0040	.0158	.0089	.0089	.0089	.0089	.0089	.0000	.0022	.0268	.0000	.0022	.0022	.0022		.0022		.0022	
Slope of radius through end of chord	0	0	0	0	0	0	0	0	0	0	0	0	0	2/10		2/20		2/10	

TABLE II

COEFFICIENTS FOR FORM EQUATIONS

Basic airfoil forms	Coefficients for equation (1)				Coefficients for equation (2)			
Design no.	a_0	a_1	a_2	a_3	d_0	d_1	d_2	d_3
0020-62	0.296900	0.213337	−2.931954	5.229170	0.002000	0.200000	−0.040625	−0.070312
0020-63	.296900	−.096082	−.543310	.569395	.002000	.234000	−.068571	−.093878
0020-64	.296900	−.246867	.175334	−.266917	.002000	.315000	−.233333	−.032407
0020-65	.296900	−.310275	.341700	−.321820	.002000	.465000	−.684000	.292000
0020-66	.296900	−.271180	.140200	−.082137	.002000	.700000	−1.662500	1.312500
0020-03	.000000	.920286	−2.801900	2.817990	.002000	.234000	−.068571	−.093878
0020-33	.148450	.412103	−1.672610	1.688690	.002000	.234000	−.068571	−.093878
0020-93	.514246	−.840115	1.110100	−1.094010	.002000	.234000	−.068571	−.093878
0020-05	.000000	.477000	−.708000	.308000	.002000	.465000	−.684000	.292000
0020-35	.148450	.083362	−.183150	−.006910	.002000	.465000	−.684000	.292000
0020-34	.148450	.193233	−.558166	.283208	.002000	.315000	−.233333	−.032407